

Article

**Design, Synthesis and Evaluation of Thiophene[3,2-d]pyrimidine
Derivatives as HIV-1 Non-nucleoside Reverse Transcriptase
Inhibitors with Significantly Improved Drug Resistance Profiles**

Dongwei Kang, Zengjun Fang, Zhenyu Li, Boshi Huang, Heng Zhang, Xueyi Lu, Haoran Xu, Zhongxia Zhou, Xiao Ding, Dirk Daelemans, Erik De Clercq, Christophe Pannecouque, Peng Zhan, and Xinyong Liu

J. Med. Chem., **Just Accepted Manuscript** • DOI: 10.1021/acs.jmedchem.6b00738 • Publication Date (Web): 19 Aug 2016

Downloaded from <http://pubs.acs.org> on August 20, 2016

Just Accepted

“Just Accepted” manuscripts have been peer-reviewed and accepted for publication. They are posted online prior to technical editing, formatting for publication and author proofing. The American Chemical Society provides “Just Accepted” as a free service to the research community to expedite the dissemination of scientific material as soon as possible after acceptance. “Just Accepted” manuscripts appear in full in PDF format accompanied by an HTML abstract. “Just Accepted” manuscripts have been fully peer reviewed, but should not be considered the official version of record. They are accessible to all readers and citable by the Digital Object Identifier (DOI®). “Just Accepted” is an optional service offered to authors. Therefore, the “Just Accepted” Web site may not include all articles that will be published in the journal. After a manuscript is technically edited and formatted, it will be removed from the “Just Accepted” Web site and published as an ASAP article. Note that technical editing may introduce minor changes to the manuscript text and/or graphics which could affect content, and all legal disclaimers and ethical guidelines that apply to the journal pertain. ACS cannot be held responsible for errors or consequences arising from the use of information contained in these “Just Accepted” manuscripts.



ACS Publications

Design, Synthesis and Evaluation of Thiophene[3,2-d]pyrimidine Derivatives as HIV-1 Non-nucleoside Reverse Transcriptase Inhibitors with Significantly Improved Drug Resistance Profiles

Dongwei Kang,[†] Zengjun Fang,^{†,‡} Zhenyu Li,[†] Boshi Huang,[†] Heng Zhang,[†] Xueyi Lu,[†] Haoran Xu,[†] Zhongxia Zhou,[†] Xiao Ding,[†] Dirk Daelemans,[§] Erik De Clercq,[§] Christophe Pannecouque,^{§,*} Peng Zhan,^{†,*} and Xinyong Liu^{†,*}

[†] *Department of Medicinal Chemistry, Key Laboratory of Chemical Biology (Ministry of Education), School of Pharmaceutical Sciences, Shandong University, 44 West Culture Road, 250012 Jinan, Shandong, PR China*

[§] *Rega Institute for Medical Research, K.U.Leuven, Minderbroedersstraat 10, B-3000 Leuven, Belgium*

[‡] *The Second Hospital of Shandong University, No. 247 Beiyuan Avenue, Jinan 250033, China.*

ABSTRACT:

We designed and synthesized a series of human immunodeficiency virus type 1 (HIV-1) non-nucleoside reverse transcriptase inhibitors (NNRTIs) with a piperidine-substituted thiophene[3,2-d]pyrimidine scaffold, employing a strategy of structure-based molecular hybridization and substituent decorating. Most of the synthesized compounds exhibited broad-spectrum activity with low (single digit) nanomolar EC₅₀ values towards a panel of wild-type (WT), single-mutant and double-mutant HIV-1 strains. Compound **27** was the most potent; compared with ETV, its antiviral efficacy was 3-fold greater against WT, 5- to 7-fold greater against Y181C, Y188L, E138K and F227L+V106A, and nearly equipotent against L100I and K103N, though somewhat weaker against K103N+Y181C. Importantly, **27** has lower cytotoxicity (CC₅₀ >227 μM) and a huge selectivity index (SI) value (ratio of

CC₅₀/EC₅₀) of >159,101. **27** also showed favorable, drug-like pharmacokinetic and safety properties in rats *in vivo*. Molecular docking studies and the structure-activity relationships provide important clues for further molecular elaboration.

INTRODUCTION

Non-nucleoside reverse transcriptase inhibitors (NNRTIs) are a component of Highly Active Antiretroviral Therapy (HAART) regimens used to treat human immunodeficiency virus type 1 (HIV-1), the main causative agent of acquired immune deficiency syndrome (AIDS),¹⁻⁵ due to their potent antiviral activity, high selectivity, modest toxicity and favorable pharmacokinetics.⁶ NNRTIs distort the enzyme's active site and perturb the alignment of the primer terminus by interacting in a noncompetitive manner with the allosteric site (NNRTIs binding pocket, NNIBP) about 10 Å distant from the polymerase active site of RT, resulting in inhibition of the reverse transcription step of HIV-1 replication.⁶ Nevirapine (**1**, NVP), delavirdine (**2**, DLV) and efavirenz (**3**, EFV) are first-generation NNRTIs for AIDS therapy, exhibiting potent anti-HIV-1 activity, but some toxicities (for example, hepatotoxicity and severe rash are associated with the use of nevirapine, while efavirenz has central nervous system side effects).⁷ However, there is a low genetic barrier for viral resistance, and drug-resistant mutants rapidly emerge, including K103N, Y181C, Y188L single mutants and K103N/Y181C double mutant (RES056); among them, K103N and Y181C are the two most prevalent mutations *in vivo*, primarily selected by nevirapine and efavirenz, and this has limited the clinical usefulness of the

1
2
3 first-generation NNRTIs.^{8,9} Second-generation NNRTIs include the recently approved
4
5
6 drugs etravirine (**4**, ETV) and rilpivirine (**5**, RPV), both of which are the members of
7
8 the diarylpyrimidine (DAPY) family.¹⁰ Another DAPY derivative, dapivirine (**6**,
9
10 TMC120) has emerged as a microbicide with great potential for the prevention of
11
12 transmission of HIV-1 infections, showing favorable pharmacokinetics when
13
14 delivered through gels or vaginal rings.¹¹ Structure-activity relationship (SAR) studies
15
16 led to the identification of three regions (**A**, **B**, **C**) of the DAPY scaffold (Figure 1).
17
18
19 The DAPY inhibitors adopt a conformationally flexible horseshoe shape in the NNIBP,
20
21 showing both torsional flexibility (“wiggling”) and repositioning and reorientation
22
23 (“jiggling”), which may serve to minimize the loss of binding stabilization caused by
24
25 mutations.¹² Consequently, they exhibit a broad spectrum of activity against wild-type
26
27 (WT) and clinically relevant HIV-1 mutant strains, with nanomolar EC₅₀ values. The
28
29 genetic barrier to emergence of drug resistance is higher than with the first-generation
30
31 NNRTIs.¹⁰ However, hypersensitivity reactions or other adverse effects have been
32
33 reported with second-generation NNRTIs.⁶ Also, although drug resistance is delayed,
34
35 it continues to emerge in patients receiving second-generation NNRTIs regimens.¹³
36
37
38 Among resistance mutations, K103N and E138K are most frequently selected by
39
40 etravirine and rilpivirine.¹⁴ Therefore, considerable effort has been directed to find
41
42 new DAPY analogues that retain activity against NNRTIs-resistant mutants, including
43
44 K103N, Y181C, Y188L and E138K.
45
46
47
48
49
50
51
52
53
54
55
56
57
58
59
60

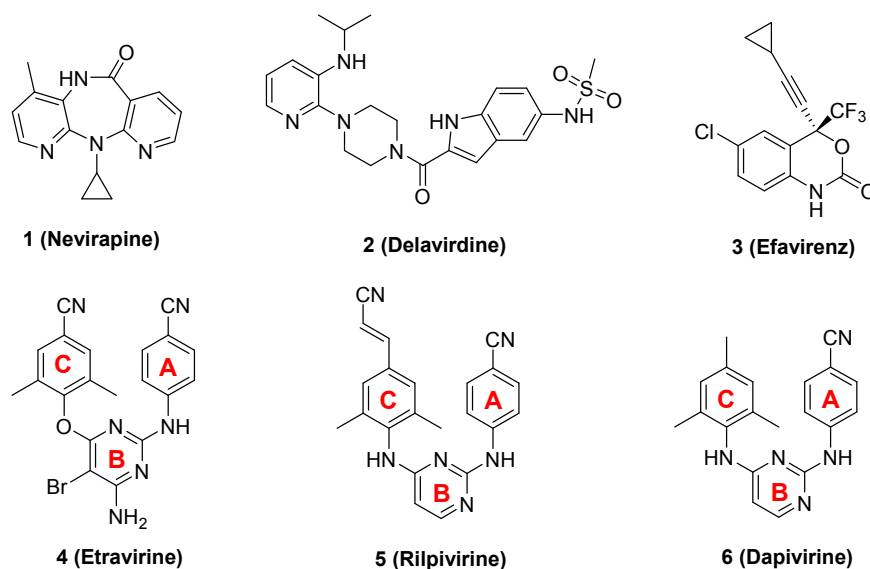


Figure 1. Chemical structures of five NNRTIs approved by the US FDA and dapivirine, a microbicide in the DAPY family.

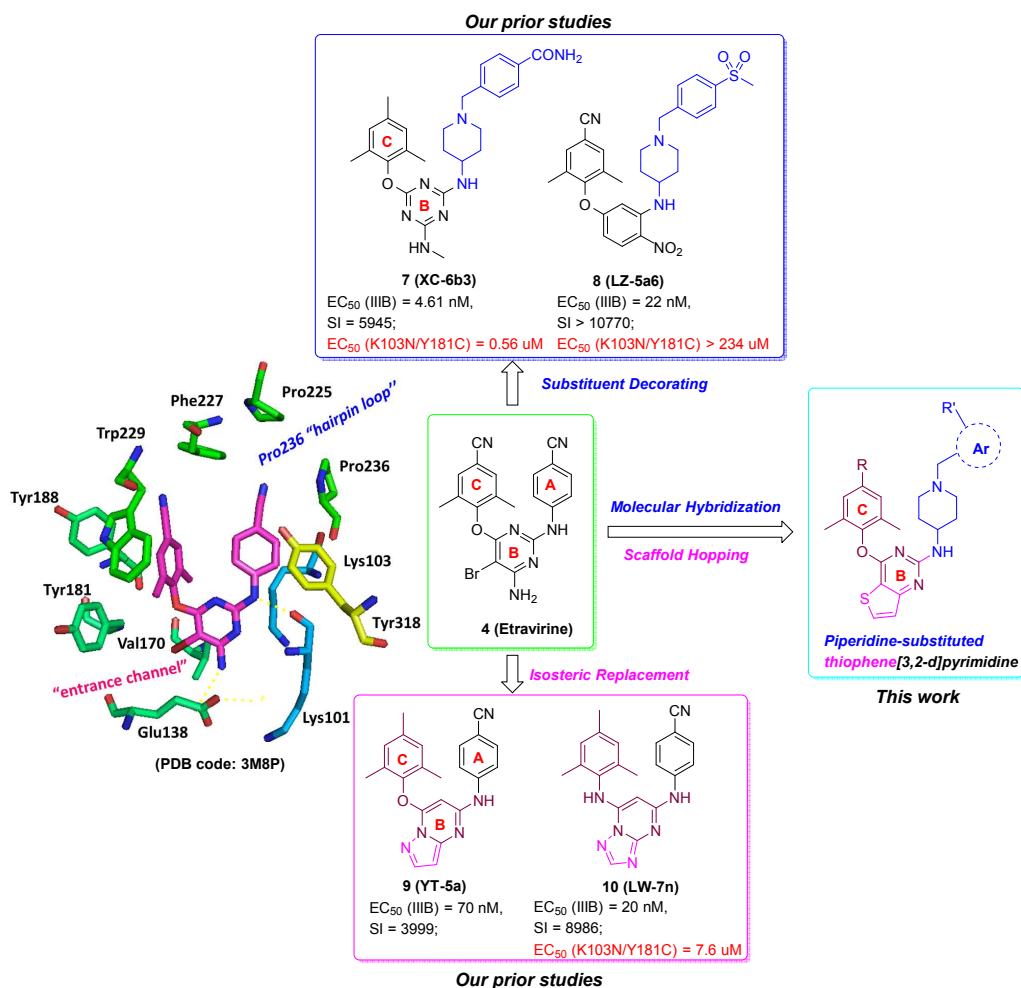


Figure 2. Design strategies used in our previous and present studies to obtain structurally elaborated DAPY-based NNRTIs utilizing the thiophene[3,2-d]pyrimidine scaffold. The illustration of the co-crystal structure of etravirine/RT was generated using PyMOL (www.pymol.org).

Detailed analysis of a wide range of crystal structures of HIV-1 RT/NNRTI complexes, together with data on drug resistance mutations, has identified several factors important for the design of NNRTIs with broad-spectrum activity against mutant HIV-1 strains;¹⁵ these factors include extensive main-chain hydrogen bonding interactions (double hydrogen-bonding chelate with the Lys101/Lys103 backbone)^{16,17} and addition of a heterocyclic motif to the parent compound to maximize interactions with highly conserved residues in the HIV-1 RT binding pocket.¹⁸

Based on the crystallographic studies, it was concluded that NNIBP contains solvent-accessible regions that provide broad regions that are potentially available to accommodate novel NNRTIs, such as tolerant region I (the Pro236 hairpin loop) and tolerant region II (the entrance channel, i.e. the largely open region in front of Lys103, Glu138 and Val179).^{15,18}

By the classical definition for drug design, an active molecule should efficiently enter and maximally occupy the binding pocket, thereby interacting effectively with the amino acids around the binding site.¹⁵ The availability of crystallographic structures of RT/DAPYs, together with the results of medicinal chemistry studies, have enabled structure-based design of various NNRTI sub-classes with promising activity profiles against mutant strains. In our lab, we have made great efforts to

utilize these two tolerant regions in the NNBIP in order to develop potent and highly selective DAPYs derivatives as antiviral agents active against the prevalent mutations in clinical HIV-1 isolates, as shown in Figure 2.

Regarding the tolerant region I, we recently reported the addition of a functionalized side tail to the known DAPY NNRTIs. The resulting piperidine-substituted triazine/aniline derivatives (exemplified by **7** (XC-6b3) and **8** (**LZ-5a6**)) showed higher potency against WT, but had only weak (**7**: $EC_{50} = 0.56 \mu M$) or no activity (**8**: $EC_{50} > 234 \mu M$) against the K103N/Y181C double mutant resistant strain.¹⁹ The aromatic *p*-cyanoaniline moiety (A-ring) in ETV and RPV was replaced with various substituted benzyl-linked piperidin-4-yl-amino moieties, as we anticipated several advantages of introducing such structures. Firstly, the N atom of the piperidine can form an additional H-bond with Lys103 through a water bridge, which might contribute to an improved resistance profiles.^{16,17} Thus, the piperidine-linked NH might serve as a Lys101/Lys103 double backbone chelate motif, because all NNRTIs can form direct or water-mediated hydrogen bonds with these amino acids in the protein backbone. Secondly, the substituted benzyls are directed toward the protein-solvent interface (the Pro236 hairpin loop) and are available to participate in additional hydrogen bonds with key residues of the NNIBP. Thirdly, the polar substituted benzyl-linked piperidin-4-yl-amino moiety could contribute to improved physicochemical and pharmacokinetic properties.²⁰

On the other hand, the entrance channel is another relatively unexplored open region in the NNIBP; this region extends into the solvent-exposed region, and is

1
2
3
4 surrounded by several relatively inflexible residues, Leu100, Lys101, Glu138 and
5
6 Val179.²¹ The entrance channel therefore represents another attractive tolerant region
7
8 that would be available to accommodate diverse groups, providing additional scope
9
10 for the generation of novel inhibitors.²²⁻²⁴
11
12

13
14 At the beginning of our endeavor to identify new DAPYs by establishing novel
15
16 binding interactions with the solvent-accessible entrance channel and to further
17
18 expand the chemical scope of the core ring system, we adopted an isosteric
19
20 replacement strategy to morph the central six-membered heterocyclic core to several
21
22 fused heterocycles bearing bridgehead nitrogen, such as pyrazolo[1,5-a]pyrimidine
23
24 and [1,2,4]triazolo[1,5-a]pyrimidine (exemplified by **9** (YT-5a) and **10** (LW-7n),
25
26 respectively). Although these representative compounds displayed potent activity
27
28 toward WT HIV-1 at low nanomolar concentrations, with high selectivity (Figure 2),
29
30 they exhibited weak potency against the K103N/Y181C double mutant HIV-1 strain
31
32 (for **10**: EC₅₀ = 7.6 μM).²⁵
33
34
35
36
37
38

39 Specific nonpolar interactions-based scaffold decoration has recently
40
41 experienced a renaissance, gaining increased recognition as a useful tool in NNRTIs
42
43 discovery.²⁶ Continuing our research project, we therefore turned our attention to the
44
45 introduction of small hydrophobic groups at the 5,6-positions in the central
46
47 pyrimidine ring of DAPY NNRTIs, aiming to establish nonpolar interactions with
48
49 hydrophobic side chains of residues in the entrance channel cleft. In the present work,
50
51 we further explored privileged and synthetically accessible piperidine-substituted
52
53 thiophene[3,2-d]pyrimidine derivatives, in which the thiophene[3,2-d]pyrimidine
54
55
56
57
58
59
60

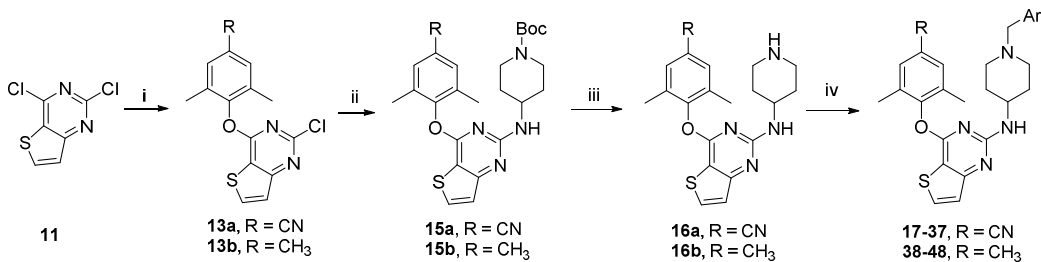
structure replaces the pyrimidine (B-ring) of the lead compound, ETV. In principle, the sulfur atom of thiophene[3,2-d]pyrimidine occupies the same position as the bromo atom of ETV. The lone-pair electrons and atomic radius ($r = 104$ pm) of the sulfur atom are similar to those of the bromo substituent of ETV ($r = 114$ pm), and there could be a strong electrostatic interaction between the thiophene[3,2-d]pyrimidine scaffold and Val179. Next, the *p*-cyanoaniline moiety (A-ring) was replaced with different substituted benzyl-linked piperidin-4-yl-amino moieties. In the resulting compounds, the piperidin-4-yl-amino and the N atom at the 1-position of the thiophene[3,2-d]pyrimidine can form multiple hydrogen bonds with the backbones of Lys101 and Lys103. The trisubstituted phenoxy ring (C-ring), which plays a crucial role in aryl-aryl interactions with Tyr181, Tyr188, Phe227 and Trp229, was retained. We expected that all these factors would allow the novel thiophene[3,2-d]pyrimidine derivatives to occupy the NNIBP more effectively, strengthening the binding interactions with residues of the NNIBP.

Thus, we report here the design and synthesis of a series of novel thiophene[3,2-d]pyrimidine derivatives with different aryl substituents varying in size, polar group substitution and electronic nature on the piperidin-4-yl-amino moiety. Anti-HIV activity evaluation showed that these compounds have potent, broad-spectrum profiles against WT and resistant mutant strains of HIV-1, being superior in these respects to the approved drug ETV. A pharmacokinetics study of the most potent compound, **27**, in rats showed that it has favorable, drug-like pharmacokinetics. Also, a detailed consideration of the SARs of this series of

derivatives suggested opportunities for further elaboration of these compounds.

CHEMISTRY

The newly designed thiophene[3,2-d]pyrimidine derivatives were synthesized according to the an efficient and reliable method, previously reported for the DAPY family,^{27,28} as outlined in Scheme 1. The synthetic work was started from commercially available 2,4-dichlorothiophene[3,2-d]pyrimidine (**11**); successive nucleophilic substitution reactions with substituted phenols (**12a** and **12b**) and 4-(*tert*-butoxycarbonyl)-aminopiperidine (**14**) in the presence of potassium carbonate and *N,N*-dimethylformamide afforded the key intermediates **15a** and **15b**. Deprotection with trifluoroacetic acid at room temperature in dichloromethane afforded the corresponding analogues **16a** and **16b**, which were led to the target compounds **17-37** and **38-48** by nucleophilic substitution with substituted benzyl chloride (or bromine) or 4-picolyl chloride hydrochloride in the presence of potassium carbonate. All new thiophene[3,2-d]pyrimidines were fully characterized by proton nuclear magnetic resonance (¹H NMR), carbon nuclear magnetic resonance (¹³C NMR), and electrospray ionisation mass spectrometry (ESI-MS). Purity of all compounds was determined to be >95% by analytical HPLC (Table S1 in Supporting Information).

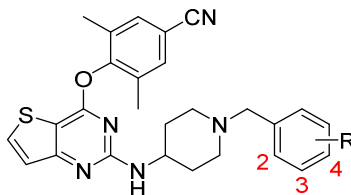


Scheme 1. Reagents and conditions: (i) substituted phenols (**12a** or **12b**), DMF, K₂CO₃, r.t.; (ii)

4-(*tert*-butoxycarbonyl)aminopiperidine (**14**), DMF, K₂CO₃, reflux, 12h; (iii) TFA, DCM, r.t.; (iv) substituted benzyl chloride (or bromine) or 4-picolyl chloride hydrochloride, DMF, K₂CO₃, r.t.

RESULTS AND DISCUSSION

Table 1. Anti-HIV activity and cytotoxicity of target compounds **17-25**



compd	R	EC ₅₀ (nM)			CC ₅₀ (nM)	SI	
		III _B	RES056	ROD		III _B	RES056
17	4-CN	5.86±3.49	440±260	>5370	5360±760	914	12
18	2-CN	5.71±2.89	810±140	>5780	5790±2410	1014	7
19	4-Br	26.56±3.94	2030±920	>24320	24320±2520	916	12
20	2-CH ₃	9.40±2.06	780±90	>10360	10360±8270	1101	13
21	3-CN	4.14±0.21	360±130	>4530	4520±310	1091	13
22	4-COOCH ₃	3.25±2.18	700±140	>41390	41390±20000	12740	59
23	3-F	4.40±2.73	290±60	>76740	76740±22030	17451	267
24	2-F	8.23±0.36	24200±18490	>189400	189400±39480	23011	8
25	4-NO ₂	7.57±0.23	520±150	>4660	4660±200	615	9
NVP	-	312±56	≥7590	-	>15020	48.08	>orX2-
3TC	-	2240±820	-	8790±2910	>87240	>39	-
AZT	-	7.1±2.9	10±9.2	6.6±1.4	>93550	>13144	>9149
EFV	-	6.02±2.0	156.1±14.9	-	>6340	>1014	>41
DLV	-	653±623	>43810	-	>43810	>67	X1
ETV	-	4.1±0.2	25.0±3.0	-	>4590	>1127	>184

^a EC₅₀: concentration of compound required to achieve 50% protection of MT-4 cell cultures against HIV-1-induced cytotoxicity, presented as the mean ± standard deviation (SD) and determined by the MTT method.

^b CC₅₀: concentration required to reduce the viability of mock-infected cell cultures by 50%, as determined by the MTT method.

^c SI: selectivity index, the ratio of CC₅₀/EC₅₀.

The first phase of our new explorations involved determining the suitability of the thiophene[3,2-d]pyrimidine core. For this purpose, we kept the 2,6-dimethyl-4-cyanophenyl structure constant in the left ring and used a small set of substituted benzyl-linked piperidin-4-yl-amino moieties as the right ring. It can be

observed that the nine newly synthesized derivatives **17-25** were evaluated for anti-HIV activity and cytotoxicity in MT-4 cell cultures infected with WT HIV-1 strain (IIIB), double-mutant strain RES056 (K103N+Y181C) and a HIV-2 strain (ROD). Nevirapine (NVP), lamivudine (3TC), delavirdine (DLV), efavirenz (EFV), etravirine (ETV) and azidothymidine (AZT) were selected as reference drugs. The values of EC_{50} , CC_{50} and SI (selectivity index, i.e., CC_{50}/EC_{50} ratio) are summarized in Table 1. All nine compounds exhibited high potency against the WT HIV-1 strain with low nanomolar EC_{50} values ranging from 3.2 to 26 nM and SI values between 615 and 23,011, which are superior to those of the reference drugs (3TC, NVP, EFV, DLV, AZT) and comparable to those of the second-generation NNRTI drug ETV. As expected, the compounds did not inhibit the HIV-2 strain. **22** turned out to be the most potent HIV-1 inhibitor with an EC_{50} value of 3.2 nM and a high SI of 12,740 in this initial assay, being slightly more potent than ETV.

The position of the substituents in the right phenyl ring has some influence on the anti-HIV activity. For instance, compounds **17-25** are basically equipotent on WT HIV with the exception of compound **19**. Specifically, addition of a cyano group at the C_2 or C_4 position in the phenyl ring (**18** and **17**) resulted in similar EC_{50} values of 5.7 nM and 5.8 nM respectively, whereas the C_3 -cyano analogue **21** had an EC_{50} value of 4.1 nM. The activity was also influenced by the electronic nature or steric demand of substituents in the right phenyl ring. For example, introduction of a nitro group at the C_4 position yielded a 7.5 nM inhibitor (**25**), while bromine at this position (**19**) reduced the potency to 26.5 nM. Placement of a methyl group at the C_2 -position

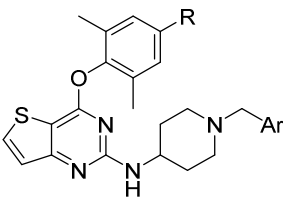
yielded **20**, which was found to have similar potency to the 2-fluoro derivative **24**.

As regards activity towards the double-mutant strain RES056, **23** was the most potent compound with an EC₅₀ value of 290 nM, which is comparable to that of EFV (EC₅₀ = 156.1 nM). It showed a moderate SI value (267) towards WT and RES056 mutant HIV-1 strains. These encouraging data provided some support for our hypothesis that introduction of thiophene[3,2-d]pyrimidine to replace the central B-ring of DAPYs would be feasible and effective. Interestingly, the 2-fluoro counterpart of **23**, i.e., **24**, showed a marked decrease of potency against RES056 mutant strain. Thus, the anti-resistance potency of the compounds is also dependent on the position of the substituents in the right phenyl ring. In addition to influencing the antiviral activity, the shapes and volumes of substituents on the right phenyl ring also had a major influence on the cytotoxicity (CC₅₀), so we continued our exploration of this fused heterocyclic motif.

Based on the preliminary SARs of these novel thienopyrimidine analogues and our previous investigations in other DAPY series, we decided to introduce some hydrophilic groups on the aryl moiety directed toward the protein-solvent interface, and we synthesized 12 new compounds (**26-37**) in the 2,6-dimethyl-4-cyanophenyl series. In addition, based on the structural characteristics of dapivirine in conjunction with previous studies,²⁴ we replaced the cyano group of the left ring with a methyl group to obtain a new 2,4,6-trimethyl-phenyl series (11 compounds, **38-48**). The anti-HIV activity of these compounds was evaluated in the MT-4 cell line against WT HIV-1 (IIIB), HIV-2 strain (ROD), and a panel of NNRTIs-resistant single- and

double-mutant strains (L100I, K103N, E138K, Y181C, Y188L, K103N+Y181C (RES056) and F227L+V106A), which are common clinical mutations in HIV-infected patients. Nevirapine (NVP), efavirenz (EFV), etravirine (ETV) and azidothymidine (AZT) were selected as reference drugs. The EC₅₀, CC₅₀ and SI values obtained are summarized in Tables 2, 3 and 4.

Table 2. Anti-HIV activity and cytotoxicity of **26-37** and **38-48**



compd	R	Ar	EC ₅₀ (nM) ^b		CC ₅₀ (nM) ^b	SI ^c
			IIIB	ROD		IIIB
26	CN	4-SO ₂ Me-Ph	22.1±11.0	>22312	22312±3453	1005
27	CN	4-SO ₂ NH ₂ -Ph	1.4±0.4	≥227890	>227890	>159101
28	CN	4-F-Ph	7.5±1.3	≥140940	140940±19443	18708
29	CN	pyridine-4-yl	10.3±1.2	>20621	20621±4744	1999
30	CN	2,4-diF-Ph	22.0±0.9	>4082	4081.8±701.2	185
31	CN	3-SO ₂ NH ₂ -Ph	2.4±1.1	>227800	>227800	>96006
32	CN	4-NHSO ₂ Me-Ph	1.5±0.3	>68266	68266±71241	44221
33	CN	4-SO ₂ NHMe-Ph	1.5±0.4	>4422	4422±1546	2789
34	CN	4-CONH ₂ -Ph	1.4±0.07	>95350	95352±27689	66867
35	CN	3-CONH ₂ -Ph	2.5±0.3	>48760	>48760	>19216
36	CN	4-COOEt-Ph	160.7±3.7	>230700	≥230700	≥1436
37	CN	4-SO ₂ NHCOMe-Ph	5.2±0.9	>3027	>3027	576
38	CH ₃	4-SO ₂ Me-Ph	5.7±1.4	>3416	3417±1043	595
39	CH ₃	4-CO ₂ Me-Ph	15.4±11.8	>24873	24873±2177	1612
40	CH ₃	4-F-Ph	25.7±12.7	>11948	11948±7041	465
41	CH ₃	3-F-Ph	39.1±6.8	>24591	24591±5262	628
42	CH ₃	3-CN-Ph	21.1±1.0	>17238	17238±6753	819
43	CH ₃	pyridine-4-yl	7.6±1.3	>5653	5653±2002	747

44	CH ₃	2,4-diF-Ph	36.8±8.8	>13958	13958±5207	380
45	CH ₃	4-CONH ₂ -Ph	6.5±2.6	>5814	5814±2294	896
46	CH ₃	3-CONH ₂ -Ph	14.4±8.6	>7638	7638±3891	531
47	CH ₃	4-SO ₂ NH ₂ -Ph	3552±848	>16460	16460±8026	2
48	CH ₃	4-NO ₂ -Ph	31.8±5.2	>6394	6394±3429	201
NVP	-	-	250±65.6	-	>15.0207	>60
EFV	-	-	5.0±02.1	-	>6.3355	>1258
ETV	-	-	4.1±0.1	-	>4.5946	>1128
AZT	-	-	5.8±4.0	-	>7.4836	>1228

^a EC₅₀: concentration of compound required to achieve 50% protection of MT-4 cell cultures against HIV-1-induced cytotoxicity, as determined by the MTT method.

^b CC₅₀: concentration required to reduce the viability of mock-infected cell cultures by 50%, as determined by the MTT method.

^c SI: selectivity index, the ratio of CC₅₀/EC₅₀.

Firstly, we will discuss the activity of the 2,6-dimethyl-4-cyanophenyl series towards WT HIV-1. These twelve newly synthesized compounds clearly showed more potent inhibition than the initial nine compounds in this series. In particular, **27** and **31-35** displayed prominent inhibitory activity with EC₅₀ values of 1.4 nM to 2.5 nM, being more potent than the reference drugs AZT (EC₅₀ = 5.8 nM), EFV (EC₅₀ = 5.0 nM) and ETV (EC₅₀ = 4.1 nM). On the other hand, **26**, **28**, **29**, **30** and **31** (EC₅₀ = 5.2 nM) were equipotent with ETV, or less potent. It was concluded that the activity is very sensitive to substitution at the *para*-position. The order of potency of the *para*-substitution at the right phenyl ring was as follows: -SO₂NH₂ (**27**, EC₅₀ = 1.4 nM) = -CONH₂ (**34**, EC₅₀ = 1.4 nM) ≈ -NH₂SO₂Me (**32**, EC₅₀ = 1.5 nM) ≈ -SO₂NHMe (**33**, EC₅₀ = 1.5 nM) ≈ -SO₂NHCOMe (**37**, EC₅₀ = 5.2 nM) > -F (**28**, EC₅₀ = 7.5 nM) > -COOEt (**36**, EC₅₀ = 160.7 nM), indicating that polar groups, such as unsubstituted sulfamide and amide, are preferred over groups with lower polarity, such as substituted sulfamide, fluorine or ester.

1
2
3
4 It was particularly noteworthy that when the -CO₂Me group of the **22** was
5
6 replaced with -CO₂Et (**36**), the increased length of the carbochain reduced the activity
7
8 about 50-fold (EC₅₀ = 160.7 nM), but **36** exhibited no cytotoxicity at the
9
10 concentration of 230 μM. Detailed comparison of the activities of **26** with **27** and **34**
11
12 with **36** suggested that a hydrogen-bond donor group at the 4-position in the phenyl
13
14 ring strengthens the interaction with the NNRTI binding site. Subsequent N-acylation
15
16 of SO₂NH₂ of **27** gave the 5.2 nM inhibitor **37**, which is as potent as the reference
17
18 drug ETV (EC₅₀ = 4.1 nM); however, **37** shows reduced activity and increased
19
20 cytotoxicity compared with **27**, suggesting that increased hydrophobicity and steric
21
22 bulk at the *para*-position impact negatively on the activity and cytotoxicity.
23
24
25
26
27
28

29 In addition, it is noteworthy that fluorine substitution at the C₄-position gave the
30
31 7.5 nM compound **28**, which is equipotent with the C₂-fluorine compound (**24**, EC₅₀ =
32
33 8.2 nM), whereas the simultaneous presence of fluorines at C₂ and C₄ in the phenyl
34
35 ring was significantly detrimental: the potency was reduced to 22 nM and the
36
37 cytotoxicity was increased 4.08 μM. On the whole, *para* substitution of the phenyl
38
39 moiety on the right ring, relative to the *meta*-position, seems favorable for antiviral
40
41 potency, as suggested by comparison of **27/31** and **34/35**.
42
43
44
45

46 The cytotoxicity is also strongly dependent on the nature of the substituents at
47
48 the *para*-position of the phenyl ring. For instance, **27** and **31** with -SO₂NH₂
49
50 substitution at C₄ and C₃ in the phenyl ring showed no cytotoxicity (CC₅₀) up to the
51
52 maximum tested concentration of 227 μM, while addition of a methyl group to
53
54 -SO₂NH₂ (**33**) sharply increased the cytotoxicity to 4.4 μM (>51.7-fold increase).
55
56
57
58
59
60

Compared to **27** and **31**, **34** and **35** bearing a -CONH₂ group showed moderate cytotoxicity. Replacement of the SO₂NH₂ group at C₄ in the phenyl ring with SO₂Me yielded **26**, which showed reduced cytotoxicity and decreased potency.

Furthermore, the pyridine derivative **29** showed an acceptable anti-HIV-1 profile, with an EC₅₀ of 10.3 nM against WT HIV-1 (Table 2). These results support the idea that introduction of structurally diverse heterocycles in this region could be a valid strategy to discover novel molecules with appreciable antiviral potency.

Next, we turned our attention to the SAR of the R substituent at the *para*-position of the left ring. The activities of the 2,4,6-trimethylphenyl series (**38-48**) were much lower than those of the 2,6-dimethyl-4-cyanophenyl series, except for **38** and **43**, which showed an improvement of EC₅₀ to 5.7 nM and 7.6 nM compared with **26** and **29**, respectively. Moreover, nearly all of the 2,4,6-trimethylphenyl series compounds exhibited higher cytotoxicity than the 2,6-dimethyl-4-cyanophenyl series. All these results indicate that the cyano group plays a key role in enhancing the antiviral potency and reducing cytotoxicity. Preliminary SAR of the *para*-substituent group in the phenyl ring indicated the following order of activity towards WT HIV-1: -SO₂Me (**38**: EC₅₀ = 5.7 nM) \approx -CO₂NH₂ (**45**: EC₅₀ = 6.5 nM) > -CO₂Me (**39**: EC₅₀ = 15.4 nM) > F (**40**: EC₅₀ = 25.7 nM) > NO₂ (**48**: EC₅₀ = 31.8 nM). **47** bearing the SO₂NH₂ substituent showed sharply weaker activity than the corresponding derivative **27**. This seems to be a good example of an activity cliff (in particular, a 3D activity cliff), where pairs of compounds with similar structure exhibit a large difference in activity profile.^{29,30} High sensitivity of the activity profile to molecular configuration

is related to the flexibility of the binding pocket and the induced-fit mechanism of the NNRTIs (vide supra).

Similarly, variation of the position of the substituent in the right ring (from the *para*-position to the *meta*-position) resulted in slightly reduced potency (**40/41**, **45/46**), which is consistent with the SAR conclusions in the 2,6-dimethyl-4-cyanophenyl series.

The activity of the synthesized derivatives was further evaluated against a panel of clinical relevant HIV-1 mutant strains, including L100I, K103N, Y181C, Y188L, E138K, F227L+V106A and RES056, in MT-4 cells. The results are summarized in Table 3. Generally speaking, compounds that displayed potent activity against WT HIV-1 virus also showed potent activity against mutant HIV-1 strains. Nearly all of the compounds in the 2,6-dimethyl-4-cyanophenyl series exhibited high potency against mutant HIV-1 replication, with nanomolar EC₅₀ values and much higher SI values than EFV, comparable to those of ETV and AZT, with the exception of **36**. Regarding the fold resistance (RF, ratio of EC₅₀ against mutant strain/EC₅₀ against WT strain), most compounds exhibited low RF values towards L100I, K103N, Y181C, Y188L, E138K and F227L+V106A, as shown in Table S2 (see Supporting Information). Indeed, the most potent compound **27** showed nearly the lowest RF value (< 3) towards these mutants with the exception of RES056, and was comparable to ETV in this regard.

Notably, derivatives with hydrophilic substituents in the phenyl ring, such as 4-SO₂NH₂, 3-SO₂NH₂, 4-NHSO₂Me, 4-SO₂NHMe, 4-SO₂NHCOMe and 4-CONH₂,

were as potent as ETV or more potent towards nearly all the mutants, with the notable exception of the 3-CONH₂ substituent (**35**, **36**), which resulted in substantially reduced antiviral activity. Replacement of hydrophilic groups in the phenyl ring with hydrophobic groups (such as **27** vs. **28**, **36**; **45** vs. **40**, **41** and **42**) markedly reduced the activity towards the mutants, as well as towards WT HIV-1 strain.

In the case of the L100I mutant HIV-1 strain, **27** and **33** exhibited potency of 3.4 nM and 4.5 nM, respectively, being far more potent than EFV, showing the same potency as ETV, and comparable to AZT. As for K103N, which is the most common mutation emerging in HIV patients treated with EFV, eleven compounds provided single-digit-nanomolar activity. In particular, **33** (EC₅₀ = 1.5 nM) was notably more active than ETV and AZT. Further, compounds **27** and **32-34** showed single-digit-nanomolar inhibitory activity towards the single mutants Y181C, Y188L and E138K, with EC₅₀ values ranging from 2.9 nM to 8.2 nM (at least 2-7 fold more potent than ETV). **31** and **37** were also highly potent inhibitors toward Y188L and E138K, with greater potency than ETV; however, both derivatives exhibited reduced inhibition of the Y181C strain. Intriguingly, seven compounds (**27**, **31-35** and **37**) in the 2,6-dimethyl-4-cyanophenyl series displayed greater potency than ETV against E138K, a major mutation conferring resistance to the new-generation drug rilpivirine (**5**, RPV). In particular, **27**, **31** and **34** had high anti-resistance potency, with RF = 2.0-3.1 for E138K.²³

Against the double-mutant strain F227L+V106A, derivatives with hydrophilic substituents in the phenyl ring were all superior to ETV, except for **32**, indicating that

1
2
3
4 4-NHSO₂Me is unfavorable for activity towards this mutant strain. Among all the
5
6 derivatives, **27** and **33** showed the greatest potency against the double mutation
7
8 RES056 (EC₅₀ = 30.6 and 32.4 nM), being slightly inferior to ETV (EC₅₀ = 17 nM),
9
10 but they were less potent towards K103N and Y181C.
11
12

13
14 However, the 2,4,6-trimethylphenyl series showed weaker activity than the
15
16 2,6-dimethyl-4-cyanophenyl series, with the exception of **38** bearing a SO₂CH₃
17
18 substituent. **38** exhibited remarkable potency against several key mutant strains.
19
20 Indeed, it turned out to be a 23.9 nM inhibitor of F227L+V106A, being more potent
21
22 than ETV. **45** was also effective against E138K. In contrast, **47** with the SO₂NH₂
23
24 substituent showed greatly reduced activity compared to **27**, which may represent
25
26 another example of the activity cliff concept. **44** with fluorine substitution at both C₂
27
28 and C₄ of the phenyl ring also showed reduced potency compared with
29
30 mono-fluorine-substituted **40** and **41**.
31
32
33
34
35

36
37 Among all the compounds examined, **27** showed outstanding antiretroviral
38
39 potency against most of the viral panel, being about 3-fold (WT, EC₅₀ = 0.14 nM),
40
41 1.6-fold (L100I, EC₅₀ = 3.4 nM), 5-fold (Y181C, EC₅₀ = 3.2 nM; E138K, EC₅₀ = 2.9
42
43 nM) and 7-fold (Y188L, EC₅₀ = 3.0 nM; F227L+V106A, EC₅₀ = 4.2 nM) more potent
44
45 than the reference drug ETV in the same cellular assay, and remarkably superior to
46
47 that of the reference drugs NVP and EFV. Importantly, **27** showed no cytotoxicity at
48
49 concentrations up to 227 μM, resulting in a huge SI value (CC₅₀/EC₅₀) of >159,101
50
51 compared with that of ETV (CC₅₀ > 4.59 μM; SI > 1128). Since this novel chemotype
52
53 has activity against a broad range of NNRTIs-resistant mutant viruses, we believe that
54
55
56
57
58
59
60

compounds of this class have enormous potential as anti-HIV drug candidates.

To validate the binding target of these novel thienopyrimidine derivatives, some representative compounds were also tested for ability to inhibit recombinant WT and K103N/Y181C double-mutant HIV-1 RT enzymes; the results are shown in Table 4. In this assay, all the tested compounds exhibited potent inhibitory activities toward WT with IC_{50} values ranging from 0.21 to 1.68 μ M, being superior to the reference drug NVP. These compounds were also comparable in potency to EFV against double-mutant RT, with the IC_{50} values ranging from 0.36 to 46.37 μ M. Generally, the SAR for inhibitory potency appeared to be consistent between HIV-1 replication and RT activity. Hydrophilic substituents on the phenyl ring were beneficial for inhibitory activities against both WT and double mutant RT (**27**, **29**, **38** and **43**).

Compound **43** with a pyridine-4-yl substituent in the phenyl ring displayed the most potent activity towards WT RT with an IC_{50} value of 0.21 μ M, while the inhibitory activity against double-mutant RT was reduced to 1.26 μ M (FR = 6.0). Another potent inhibitor of WT RT (IC_{50} = 0.30 μ M), the C_4 -SO₂NH₂ derivative **27**, also showed more potent inhibitory activity against double-mutant RT than the reference drug EFV, and it also showed a low FR value (1.20) with respect to WT RT. It seems that the binding mode of **27** was not affected by the K103N/Y181C mutation and was consistent with the interactions reported for the WT strain. These results demonstrated that representative compounds displayed high affinity for WT and double-mutant HIV-1 RT, and support the view that the target of the newly synthesized compounds is HIV-1 RT.

It is noteworthy that the antiviral activities of the best compounds in this study (the pyridine-4-yl **43** and the sulfonamide **27**) were inconsistent with their enzyme-inhibitory potencies to some extent. These differences are considered to be due to template-specific variation in the relationship between HIV-RT-RNA binding affinity and polymerase processivity, and have been observed in most NNRTI series.³¹ Besides, since these molecules have multiple hydrogen bond donor and acceptor sites, there is a high probability of formation of cocrystals or salts. Therefore, the differences between the two assay systems can be attributed at least in part to differences in the physiochemical properties (especially the intrinsic solubility).

Table 4. Inhibitory activity of compounds **26-29**, **38-44** against HIV-1 RT (WT and K103N/Y181C double mutant).

Compd	Ar	IC ₅₀ (μM) ^a (fold resistance) ^b	
		WT	K103N/Y181C double mutant
26	4-SO ₂ Me-Ph	1.51±0.09 (1)	2.83±0.39 (1.87)
27	4-SO ₂ NH ₂ -Ph	0.30±0.06(1)	0.36±0.06 (1.20)
28	4-F-Ph	0.81±0.06 (1)	2.57±0.16 (3.17)
29	pyridine-4-yl	1.30±0.22 (1)	3.74±0.06 (2.87)
38	4-SO ₂ Me-Ph	0.65±0.08 (1)	2.50±0.40 (3.84)
39	4-CO ₂ Me-Ph	1.24±0.15 (1)	12.3±0.21 (9.92)
40	4-F-Ph	1.23±0.07 (1)	6.57±1.80 (5.34)
41	3-F-Ph	0.79±0.02 (1)	40.4±25.3 (51.2)
42	3-CN-Ph	1.06±0.01 (1)	5.57±0.67 (5.25)
43	pyridine-4-yl	0.21±0.01 (1)	1.26±0.27 (6.0)
44	2,4-diF-Ph	1.6±0.21 (1)	46.37± 5.18(30.0)
NVP	-	2.32 (1)	-
EFV	-	0.03 (1)	1.42 (47.3)
ETV	-	0.011±0.000 ^c	0.09

^aIC₅₀: inhibitory concentration of test compound required to inhibit biotin deoxyuridine triphosphate (biotin-dUTP) incorporation into HIV-1 (WT, K103N/Y181C double mutant) RT by 50%.

^bfold resistance (FR): IC₅₀(K103N/Y181C mutant RT)/IC₅₀(WT RT) ratio.

^cThe data were obtained from the same laboratory (Prof. Erik De Clercq, Rega Institute for Medical Research, K.U. Leuven, Belgium).^{25e}

MOLECULAR MODELING STUDIES

To obtain further insight into the allosteric binding of the thienopyrimidine derivatives to the NNIBP of RT and to gain a deeper understanding of key structural aspects of their interaction, we performed molecular docking studies for representative compounds **27**, **32**, **33**, **34** and **43** by using the software SurflexeDock SYBYL-X 2.0. Docking results were visualized with PyMOL. The starting point to establish the most suitable settings for docking experiments was the crystallographic structure of the co-crystal of WT RT with an analogue (PDB ID: 3M8Q). The docking protocol is described in the computational section.

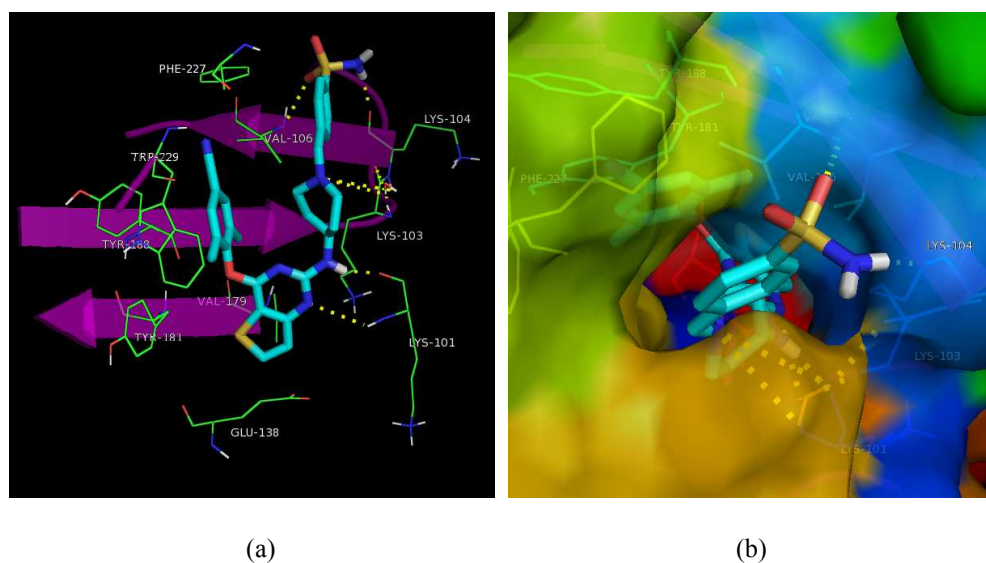


Figure 3. Predicted binding modes of **27** with the HIV-1 WT RT crystal structure (PDB: 3M8Q).

(a) Overview; (b) View looking inward along the enzyme-solvent interface (tolerant region I, the Pro236 hairpin loop), showing the solvent-exposed lower surface of the benzene sulfonamide group in **27**. The hydrogen bonds between the inhibitors and amino acid residues are indicated with dashed lines (yellow). Ligand carbon atoms are shown in cyan, and protein carbon atoms in green. Hydrogen atoms are not shown for clarity.

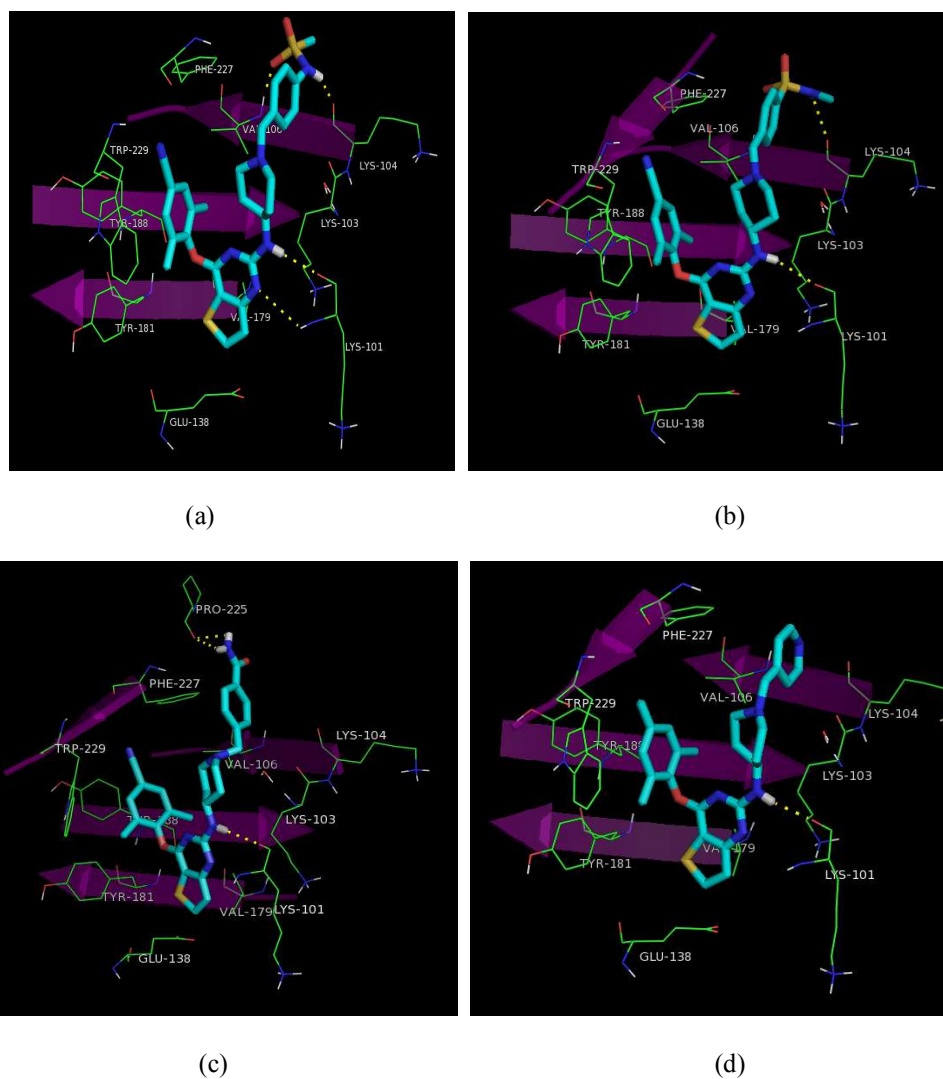


Figure 4. Predicted binding modes of **32** (a), **33** (b), **34** (c) and **43** (d) with the HIV-1 WT RT crystal structure (PDB: 3M8Q). The hydrogen bonds between the inhibitors and amino acid residues are indicated with dashed lines (yellow). Ligand carbon atoms are shown in cyan, and protein carbon atoms in green. Hydrogen atoms are not shown for clarity.

The docking simulations of these molecules with HIV-1 WT RT indicated that the binding mode resembles those of known and approved NNRTI drugs (Figure 3 and 4). In particular, the SYBYL-X 2.0-predicated binding mode of these compounds resembles that of known and approved NNRTI drugs of the DAPY family. Detailed computational analysis of the pharmacophoric interactions revealed the following

features. Firstly, the left 4-cyano-2,6-dimethylphenyl or 2,4,6-trimethylphenyl group of these compounds occupies the sub-pocket formed by hydrophobic aromatic amino acid residues Tyr181, Tyr188, Phe227 and Trp229, exhibiting π - π interaction with these residues. Secondly, the thiophene[3,2-d]pyrimidine heterocycle effectively occupies the NNIBP entrance channel, and the sulphur atom of the thiophene heterocycle has an electrostatic interaction with Val179. Thirdly, the NH linker connecting the central pyridine ring and the right ring forms the “signature” hydrogen bond with the main-chain backbone of Lys101, as seen with many NNRTIs. Fourthly, the piperidine-linked aryl structure is directed to the protein-solvent interface, and can develop extensive interactions with surrounding lipophilic amino acids, thereby improving the stability of the RT-inhibitor complex. Notably, the hydrophilic sulfonyl group of **27** or methanesulfonamide of **32** (Figure 4a) provides two hydrogen-bond receptors, thus enabling double hydrogen-bonding (chelate type) interactions with the main chain of Lys104 and Val106, which would increase the stability of the RT/NNRTI complex; In addition, the NH of the N-methylbenzenesulfonamide group in **33** (Figure 4b) participates in one hydrogen bond with the backbone C=O group of Lys104. Compared with **32**, the disappeared hydrogen bond between **33** and Val106 may explain the very distinct inhibition profile against F227L+V106A mutant strain ($EC_{50} = 4.1$ nM), which is much better than that of **32** ($EC_{50} = 32.2$ nM), probably because the binding mode of **33** was slightly altered by the V106A mutation. In contrast, the pyridine ring in **34** does not establish any hydrogen bond interactions with residues in the enzyme-solvent interface, in accordance with the eclipsed

anti-resistance profiles (Table 4). More importantly, only for **27**, additional hydrogen-bond(s) were formed with a bridging water molecule. This provides a rational explanation of the improved inhibitory potency of **27** towards WT and drug-resistant HIV-1 mutant strains, as compared with ETV (Figure 2) and the other four counterparts (Figure 4a-d). The combination of the above four features is unique to **27**, and this may be the reason why **27** possessed the most potent activity against WT and mutant HIV-1 strains.

In summary, the docking simulations indicated that **27** appears to have achieved the binding mode and the key pharmacophoric interactions that we had targeted in our original design. Further optimization of back-up derivatives is in progress, guided by these docking simulation results.

IN VIVO PHARMACOKINETICS STUDY AND SAFETY ASSESSMENT

To examine the drug potential of **27**, we evaluated the single-dose oral pharmacokinetics of **27** in rats after at two dosage levels (8 and 16 mg.kg⁻¹). As shown in Table 5 and Figure 5, the pharmacokinetics of **27** is characterized by a large volume of distribution (V_z/F of 38.2 and 50.1 L/kg), fast T_{max} (1 h, 0.8 h), moderate plasma clearance (CL_z/F of 10.3 and 9.3 L/h/kg), favorable half-life (t_{1/2} of 2.51 h and 3.60 h) and mean residence time (MRT) of 7.7 h and 9.29 h at these two dose levels. All these results indicate that **27** as an orally bioavailable candidate for clinical treatment of human HIV-1 infection.

Single dose toxicity test of compound **27** was carried out in mice. After intragastric administration of **27** with a dose of 2000 mg/kg, no death of the mice was

observed and there was no abnormality of the body weight increase for the animals in one weeks.

Table 5. Main pharmacokinetic parameters of **27**^a

Parameter	Unit	8 mg/kg	16 mg/kg
AUC(0-t)	µg/L*h	1675.8±517.0	1668.8±348.1
AUC(0-∞)	µg/L*h	1720.9±513.9	1756.7±325.1
AUMC(0-t)		5690.8±1589.3	5458.8±1341.0
AUMC(0-∞)		6474.1±1574.9	7215.795±1278.4
MRT(0-t)	h	3.44±0.46	3.25±0.19
MRT(0-∞)	h	3.84±0.51	4.16±0.79
VRT(0-t)	h ²	7.78±1.43	9.29±1.32
VRT(0-∞)	h ²	13.31±2.96	25.29±18.57
t _{1/2} Z	h	2.51±0.34	3.60±1.12
T _{max}	h	1±0.61	0.8±0.27
CL _Z /F	L/h/kg	10.3±4.3	9.3±1.8
V _Z /F	L/kg	38.2±19.2	50.1±24.7
C _{max}	µg/L	415.1±160.6	471.9±114.8

^aPK parameters (Mean ± SD, n =5).

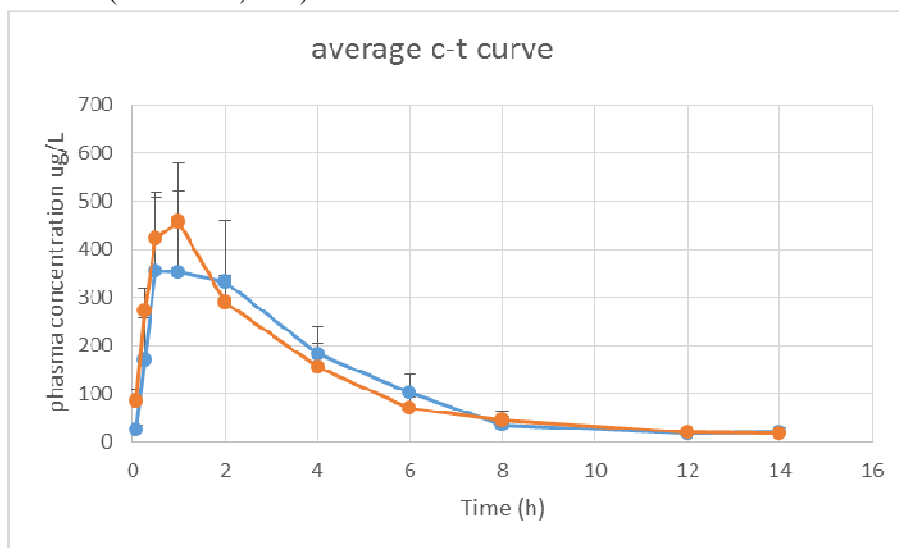


Figure 5. The plasma concentration–time profiles of **27** in rats following single oral administration at doses of 8 mg.kg⁻¹ (blue) and 16 mg.kg⁻¹ (red).

CONCLUSION

By exploiting the tolerated regions of the NNIBP, and employing a strategy of structure-based scaffold hopping and molecular hybridization, we identified a series of new piperidine-linked thiophene[3,2-d]pyrimidine derivatives having various substituents at the secondary amine of the piperidine as highly potent HIV-1 inhibitors. Most of the synthesized compounds exhibited significant inhibitory activity towards WT HIV-1 strain in MT-4 cells ($EC_{50} < 10$ nM). Among them, **17**, **20-23** and **27** exhibited high potency towards WT, with EC_{50} values of less than 5 nM and were as potent as, or more potent than, the new NNRTI drug ETV. As for RT HIV-1 mutant strains, **27-30**, **38** and **43** showed comparable inhibitory activities to those of EFV against L100I, K103N, Y188L and F227L+V106A. Notably, seven compounds (**27**, **31-35** and **37**) in the 2,6-dimethyl-4-cyanophenyl series displayed greater potency than ETV against E138K, a major viral mutation conferring resistance to the new-generation drug rilpivirine. **38** and **43** exhibited similar inhibitory activities to ETV against E138K. **27** proved to be exceptionally potent, with EC_{50} values of 1.4 nM (WT), 3.4 nM (L100I), 2.9 nM (K103N), 3.2 nM (Y181C), 3.0 nM (Y188L), 2.9 nM (E138K), 4.2 nM (F227L+V106A), and 30.6 nM (RES056) in MT-4 cells; it was more potent than ETV against all these strains except RES056. **27** also has much lower cytotoxicity ($CC_{50} > 227$ μ M) and a dramatically higher SI value of $>159,101$. In addition, **27** displayed greater inhibitory activities than NVP and EFV against recombinant WT and K103N/Y181C double-mutant RT enzymes in RT inhibition assay. **27** was confirmed to show favorable, drug-like pharmacokinetic properties in single-dose administration studies in rats. Overall, our results indicate that **27** holds

great promise as a potential next-generation anti-HIV drug candidate with significantly improved activity, high selectivity, an outstanding drug resistance profiles and favorable pharmacokinetic and safety profile.

Molecular docking experiments suggested that the strong activity profile of **27** against WT and mutant HIV-1 strains can be attributed at least in part to H-bond interactions between the hydrophilic sulfonyl group of **27** and the main chain of Lys104 and Val106, together with the nonpolar interaction between the sulphur atom of the thiophene heterocycle and Val179. These results are in accordance with established SAR data and the experimental findings with the panel of WT and mutant HIV-1 strains. Generally, it seems likely that the extensive network of main-chain hydrogen bonds is unlikely to be disrupted by side chain mutations and contributes substantially to the free energy of binding for the inhibitor, and lastly, significantly improves the resistance profiles of these inhibitors. Therefore, this important design concept targeting the main chain of a protein and forming additional key interactions indeed offers a reliable strategy for combating drug resistance. We consider that these thiophene[3,2-d]pyrimidine compounds are exciting outcomes of the simultaneous exploitation of tolerated regions I and II of NNIBP. Our findings also provide useful clues to specific interactions that could be utilized in the design of future HIV-1 NNRTIs. We believe that the thiophene[3,2-d]pyrimidine scaffold can be further optimized by adjusting the substitution at thiophene, and we are currently focusing our further medicinal chemistry efforts on this area.

EXPERIMENTAL SECTION

Chemistry

All melting points were determined on a micro melting point apparatus (RY-1G, Tianjin TianGuang Optical Instruments) and are uncorrected. ^1H -NMR and ^{13}C -NMR spectra were recorded in CDCl_3 or $\text{DMSO}-d_6$ on a Bruker AV-400 spectrometer with tetramethylsilane (TMS) as the internal standard. Coupling constants are given in hertz, and chemical shifts are reported in δ values (ppm) from TMS; signals are abbreviated as s (singlet), d (doublet), t (triplet), q (quarter), and m (multiplet). A G1313A Standard LC Autosampler (Agilent) was used to collect samples for measurement of mass spectra. The temperature of the reaction mixture was monitored with a mercury thermometer. All reactions were routinely monitored by thin layer chromatography (TLC) on Silica Gel GF254 for TLC (Merck), and spots were visualized with iodine vapor or by irradiation with UV light ($\lambda = 254 \text{ nm}$). After completion of each reaction, the mixture was brought to room temperature by means of air-jet cooling. Flash column chromatography was performed on columns packed with Silica Gel (200-300 mesh), purchased from Qingdao Haiyang Chemical Company. Solvents were of reagent grade and were purified and dried by means of standard methods when necessary. Organic solutions were dried over anhydrous sodium sulfate and concentrated with a rotary evaporator under reduced pressure. Other reagents were obtained commercially and were used without further purification. Analysis of sample purity was performed on a Shimadzu SPD-20A/20AV HPLC system with a Inertsil ODS-SP, $5 \mu\text{m}$ C18 column ($150 \text{ mm} \times 4.6 \text{ mm}$). HPLC conditions: methanol/water with 0.1% formic acid 80:20; flow rate 1.0 mL/min; UV

detection from 210 to 400 nm; temperature, ambient; injection volume, 10 μ L.

4-((2-Chlorothieno[3,2-d]pyrimidin-4-yl)oxy)-3,5-dimethylbenzonitrile (13a). A reaction mixture of 4-hydroxy-3,5-dimethylbenzonitrile (**12a**, 0.15 g, 1 mmol) and potassium carbonate (0.17 g, 1.2 mmol) in 3 mL of DMF was stirred at 25°C for 15 min, and then 2,4-dichlorothiopheno[3,2-d]pyrimidine (**11**, 0.21 g, 1 mmol) was added to it. Stirring was continued for an additional 2 h (monitored by TLC), then the mixture was poured into ice water and left to stand for 1h. The precipitated white solid was collected by filtration, washed with cold water, and recrystallized in DMF-H₂O to provide the desired product **13a** as a white solid in 93.8 % yield, mp: 258-260°C. ESI-MS: m/z 416.3 (M+1). C₁₅H₁₀ClN₃OS (315.02).

2-Chloro-4-(mesityloxy)thieno[3,2-d]pyrimidine (13b). The synthetic method was similar to that described for of **13a**, but starting from 2,4,6-trimethylphenol (**12b**, 0.14 g, 1 mmol). White solid, 96.1% yield, mp: 195-197°C. ESI-MS: m/z 416.3 (M+1). C₁₅H₁₃ClN₂OS (304.04).

3,5-Dimethyl-4-((2-(piperidin-4-ylamino)thieno[3,2-d]pyrimidin-4-yl)oxy)benzonitrile (16a). A solution of **13a** (0.32 g, 1.0mmol), *N*-Boc-4-aminopiperidine (**14**, 0.24 g, 1.2 mmol), and anhydrous K₂CO₃ (0.28 g, 2 mmol) in 5 mL of DMF was heated at 120°C under magnetic stirring for 12 h. The solution was cooled to room temperature and 10 mL of ice water was added to it. The resulting precipitate was collected by filtration, and dried to give crude **15a**, which was used directly in the next step without further purification. To a solution of **15a** (0.60 g, 1.21 mmol) in dichloromethane (DCM) (4 mL) was added trifluoroacetic acid (TFA) (0.74 mL, 10

mmol) at room temperature, and the solution was stirred for 3 h (monitored by TLC). Then, the reaction solution was alkalized to pH 9 with saturated sodium bicarbonate solution and washed with water (10 mL). The aqueous phase was extracted with DCM (3×5 mL). The combined organic phase was dried over anhydrous Na₂SO₄, filtered and concentrated under reduced pressure to give **16a** as a white solid in 84.2% yield, mp: 114-116°C. ¹H NMR (400 MHz, DMSO-*d*₆, ppm) δ: 8.20 (d, *J* = 5.4 Hz, 1H), 7.72 (s, 1H), 7.26 (s, 1H), 6.92 (s, 1H), 3.78 (s, 1H), 2.89 (s, 2H), 2.12 (s, 6H), 1.74-1.78 (m, 2H), 1.23-1.28 (m, 4H). ESI-MS: *m/z* 380.5 (M+1). C₂₀H₂₁N₅OS (379.15).

4-(Mesityloxy)-N-(piperidin-4-yl)thieno[3,2-d]pyrimidin-2-amine (16b). The synthetic method was similar to that of **16a** and starting with material **13b** (0.31g, 1.0mmol). White solid, 87.5% yield, mp: 178-180°C. ¹H NMR (400 MHz, CDCl₃, ppm) δ: 7.73 (d, *J* = 5.4 Hz, 1H, C₆-thienopyrimidine-H), 7.19 (d, *J* = 5.3 Hz, 1H, C₇-thienopyrimidine-H), 6.90 (s, 2H, C₃,C₅-Ph''-H), 4.89 (d, *J* = 7.4 Hz, 1H, NH), 3.77 (s, 1H, NH), 3.20 (d, *J* = 12.6 Hz, 2H), 2.74-2.76 (m, 2H), 2.32 (s, 3H, C₄-Ph''-CH₃), 2.04-2.09 (m, 9H), 1.46-1.54 (m, 2H). ESI-MS: *m/z* 369.5 (M+1). C₂₀H₂₄N₄OS (368.17).

General procedure for the preparation of final compounds 17-37 and 38-48.

Compounds **16a** or **16b** were dissolved in anhydrous DMF (10 mL) in the presence of anhydrous K₂CO₃ (1.2 equal), followed by addition of appropriate substituted benzyl chloride (bromine) (1.1eq). The reaction mixture was stirred at room temperature overnight. The solvent was removed under reduced pressure, and then water (30 mL)

was added. Extracted with ethyl acetate (3×10 mL), and the organic phase was washed with saturated sodium chloride (10 mL), then dried over anhydrous Na₂SO₄ to give the corresponding crude product, which was purified by flash column chromatography and recrystallized from Ethyl acetate (EA)/petroleum ether (PE) to afford the target compounds **17-37** and **38-48**.

4-((2-((1-(4-Cyanobenzyl)piperidin-4-yl)amino)thieno[3,2-d]pyrimidin-4-yl)oxy)-3,5-di-methylbenzonitrile (17). Recrystallized from EA/PE as a white solid, 73.5% yield, mp: 97-100°C. ¹H NMR (400 MHz, DMSO-*d*₆, ppm): δ 8.20 (d, *J* = 4.0 Hz, 1H, C₆-thienopyrimidine-H), 7.79 (d, *J* = 7.7 Hz, 2H, C₃,C₅-Ph'-H), 7.72 (s, 2H, C₃,C₅-Ph''-H), 7.49 (d, *J* = 7.5 Hz, 2H, C₂,C₆-Ph'-H), 7.26 (s, 1H, C₇-thienopyrimidine-H), 6.90 (s, 1H, NH), 3.74 (s, 1H), 3.52 (s, 2H, N-CH₂), 2.73 (d, *J* = 10.5 Hz, 2H), 2.11 (s, 6H), 1.78 (s, 2H), 1.65-1.72 (m, 2H), 1.38-1.42 (m, 2H). ¹³C NMR (100 MHz, DMSO-*d*₆): δ 167.4, 162.5, 160.5, 153.5, 145.2, 136.7, 133.2, 131.9, 129.9, 129.1, 123.6, 119.3, 119.0, 110.1, 109.0, 65.4, 61.9, 52.6, 31.7, 30.4, 19.1, 16.2. ESI-MS: *m/z* 495.5 (M+1), 517.6 (M+Na). C₂₈H₂₆N₆OS (494.19). HPLC purity: 99.19%.

4-((2-((1-(2-Cyanobenzyl)piperidin-4-yl)amino)thieno[3,2-d]pyrimidin-4-yl)oxy)-3,5-di-methylbenzonitrile (18). Recrystallized from EA/PE as a white solid, 76.2% yield, mp: 85-87°C. ¹H NMR (400 MHz, DMSO-*d*₆, ppm): δ 8.20 (d, *J* = 5.3 Hz, 1H, C₆-thienopyrimidine-H), 7.80 (d, *J* = 7.9 Hz, 1H, C₆-Ph'-H), 7.72 (s, 2H, C₃,C₅-Ph''-H), 7.68 (d, *J* = 7.6 Hz, 1H, C₃-Ph'-H), 7.56 (dd, *J* = 14.8, 7.2 Hz, 1H, C₄-Ph'-H), 7.46 (dd, *J* = 14.8, 7.2 Hz, 1H, C₅-Ph'-H), 7.26 (s, 1H,

C₇-thienopyrimidine-H), 6.91 (s, 1H, NH), 3.76 (s, 1H), 3.60 (s, 2H, N-CH₂), 2.74-2.78 (m, 2H), 2.11 (s, 6H), 1.76-1.82 (m, 2H), 1.39-1.44 (m, 4H). ¹³C NMR (100 MHz, DMSO-*d*₆): δ 162.5, 153.4, 142.8, 140.1, 136.7, 135.6, 133.4, 132.9, 130.5, 128.3, 125.5, 119.0, 118.1, 112.5, 109.0, 60.3, 52.6, 31.6, 16.2. ESI-MS: *m/z* 495.5 (M+1), 517.6 (M+Na). C₂₈H₂₆N₆OS (494.19). HPLC purity: 99.80%.

4-((2-((1-(4-Bromobenzyl)piperidin-4-yl)amino)thieno[3,2-d]pyrimidin-4-yl)oxy)-3,5-di-methylbenzonitrile (19). Recrystallized from EA/PE as a white solid, 72.1% yield, mp: 126-128°C. ¹H NMR (400 MHz, DMSO-*d*₆, ppm): δ 8.20 (d, *J* = 5.3 Hz, 1H, C₆-thienopyrimidine-H), 7.72 (s, 2H, C₃,C₅-Ph''-H), 7.50 (d, *J* = 8.3 Hz, 2H, C₃,C₅-Ph'-H), 7.33 (d, *J* = 8.4 Hz, 1H, C₇-thienopyrimidine-H), 7.24 (d, *J* = 6.6 Hz, 2H, C₂,C₆-Ph'-H), 6.88 (s, 1H, NH), 3.71 (s, 1H), 3.39 (s, 2H, N-CH₂), 2.71 (s, 2H), 2.11 (s, 6H), 2.07 (s, 1H), 1.75 (s, 2H), 1.39-1.44 (m, 4H). ¹³C NMR (100 MHz, DMSO-*d*₆): δ 166.0, 162.5, 160.5, 152.0, 143.5, 138.6, 136.7, 136.1, 133.2, 131.8, 131.4, 131.3, 130.6, 129.0, 121.6, 120.2, 119.0, 109.0, 65.1, 61.7, 52.6, 31.7, 29.0, 21.1, 16.2. ESI-MS: *m/z* 548.5 (M+1), 550.5 (M+3). C₂₇H₂₆BrN₅OS (547.10). HPLC purity: 98.98%.

3,5-Dimethyl-4-((2-((1-(2-methylbenzyl)piperidin-4-yl)amino)thieno[3,2-d]pyrimidin-4-yl)oxy)benzonitrile (20). Recrystallized from EA/PE as a white solid, 65.7% yield, mp: 171-173°C. ¹H NMR (400 MHz, DMSO-*d*₆, ppm): δ 8.20 (d, *J* = 5.3 Hz, 1H, C₆-thienopyrimidine-H), 7.72 (s, 2H, C₃,C₅-Ph''-H), 7.23 (m, 2H), 7.13 (m, 3H), 6.87 (s, 1H, NH), 3.73 (s, 1H), 3.60 (s, 2H, N-CH₂), 2.72 (s, 2H), 2.30 (s, 3H), 2.11 (s, 6H), 1.99-2.02 (m, 1H), 1.76 (s, 2H), 1.39-1.44 (m, 3H). ¹³C NMR (100

MHz, DMSO-*d*₆): δ 162.3, 160.5, 153.4, 137.4, 137.1, 133.2, 132.8, 130.4, 129.9, 129.3, 128.7, 127.2, 126.2, 125.8, 119.0, 109.0, 64.4, 60.6, 52.9, 31.8, 19.2, 16.2.

ESI-MS: *m/z* 484.6 (M+1). C₂₈H₂₉N₅OS (483.21). HPLC purity: 96.26%.

4-((2-((1-(3-Cyanobenzyl)piperidin-4-yl)amino)thieno[3,2-d]pyrimidin-4-yl)oxy)-3,5-di-methylbenzonitrile (21). Recrystallized from EA/PE as a white solid, 76.1% yield, mp: 198-200°C. ¹H NMR (400 MHz, DMSO-*d*₆, ppm): δ 8.20 (d, *J* = 5.3 Hz, 1H, C₆-thienopyrimidine-H), 7.73 (m, 4H), 7.64 (d, *J* = 9.4 Hz, 1H, C₆-Ph'-H), 7.54 (t, *J* = 7.7 Hz, 1H, C₄-Ph'-H), 7.26 (s, 1H, C₇-thienopyrimidine-H), 6.90 (s, 1H, NH), 3.73 (s, 1H), 3.48 (s, 2H, N-CH₂), 2.72 (s, 2H), 2.12 (s, 6H), 2.00 (s, 1H), 1.78 (s, 2H), 1.40-1.43 (m, 3H). ¹³C NMR (100 MHz, DMSO-*d*₆): δ 162.5, 160.5, 153.4, 140.9, 136.6, 134.0, 133.2, 132.8, 132.4, 131.2, 129.8, 123.6, 119.3, 119.0, 111.6, 109.0, 61.5, 60.2, 52.6, 31.7, 21.2, 16.2. ESI-MS: *m/z* 495.5 (M+1), 517.6 (M+Na). C₂₈H₂₆N₆OS (494.19). HPLC purity: 98.26%.

Methyl 4-((4-((4-(4-cyano-2,6-dimethylphenoxy)thieno[3,2-d]pyrimidin-2-yl)amino)piperidin-1-yl)methyl)benzoate (22). Recrystallized from EA/PE as a white solid, 73.6% yield, mp: 188-191°C. ¹H NMR (400 MHz, DMSO-*d*₆, ppm): δ 8.20 (d, *J* = 5.2 Hz, 1H, C₆-thienopyrimidine-H), 7.92 (d, *J* = 8.0 Hz, 2H, C₃,C₅-Ph'-H), 7.72 (s, 2H, C₃,C₅-Ph''-H), 7.43 (d, *J* = 8.0 Hz, 2H, C₂,C₆-Ph'-H), 7.26 (s, 1H, C₇-thienopyrimidine-H), 6.90 (s, 1H, NH), 3.85 (s, 3H, COOCH₃), 3.73 (s, 1H), 3.50 (s, 2H, N-CH₂), 2.73 (s, 2H), 2.11 (s, 6H), 2.00-2.04 (m, 2H), 1.77 (s, 2H), 1.40-1.44 (m, 2H). ¹³C NMR (100 MHz, DMSO-*d*₆): δ 166.6, 162.5, 160.6, 153.5, 144.9, 133.2, 132.8, 129.5, 129.3, 128.7, 128.2, 123.5, 119.0, 109.0, 62.1, 60.2, 52.76, 52.4, 31.7,

16.2. ESI-MS: m/z 528.5 (M+1), 550.6 (M+Na). $C_{29}H_{29}N_5O_3S$ (527.20). HPLC purity: 99.28%.

4-((2-((1-(3-Fluorobenzyl)piperidin-4-yl)amino)thieno[3,2-d]pyrimidin-4-yl)oxy)-3,5-di-methylbenzonitrile (23). Recrystallized from EA/PE as a white solid, 76.4% yield, mp: 132-135°C. 1H NMR (400 MHz, DMSO- d_6 , ppm): δ 8.20 (d, J = 5.1 Hz, 1H, C₆-thienopyrimidine-H), 7.72 (s, 2H, C₃,C₅-Ph''-H), 7.36 (dd, J = 14.0, 7.2 Hz, 1H, C₅-Ph'-H), 7.27 (s, 1H, C₇-thienopyrimidine-H), 7.09-7.12 (m, 3H, Ph'-H), 6.90 (s, 1H, NH), 3.74 (s, 1H), 3.43 (s, 2H, N-CH₂), 2.73 (s, 2H), 2.12 (s, 6H), 2.00-2.04 (m, 1H), 1.78 (s, 2H), 1.40-1.44 (m, 3H). ^{13}C NMR (100 MHz, DMSO- d_6): δ 165.8, 163.9, 162.5, 161.4, 160.5, 153.4, 142.2 (d, J = 7.0 HZ), 136.7, 133.2, 132.8, 130.4, 125.0, 119.0, 115.6 (d, J = 20.0 HZ), 114.1 (d, J = 20.0 HZ), 109.0, 61.9, 52.6, 31.7, 16.2. ESI-MS: m/z 488.5 (M+1), 510.6 (M+Na). $C_{27}H_{26}FN_5OS$ (487.18). HPLC purity: 95.78%.

4-((2-((1-(2-Fluorobenzyl)piperidin-4-yl)amino)thieno[3,2-d]pyrimidin-4-yl)oxy)-3,5-di-methylbenzonitrile (24). Recrystallized from EA/PE as a white solid, 75.3% yield, mp: 158-160°C. 1H NMR (400 MHz, DMSO- d_6 , ppm): δ 8.20 (d, J = 5.2 Hz, 1H, C₆-thienopyrimidine-H), 7.71 (s, 2H, C₃,C₅-Ph''-H), 7.30-7.32 (m, 3H), 7.17 (dd, J = 14.4, 9.2 Hz, C₄,C₅-Ph'-H), 6.88 (s, 1H, NH), 3.71 (s, 1H), 3.48 (s, 2H, N-CH₂), 2.75 (s, 2H), 2.11 (s, 6H), 2.02 (s, 1H), 1.76 (s, 2H), 1.39-1.44 (m, 3H). ^{13}C NMR (100 MHz, DMSO- d_6): δ 166.0, 162.4, 160.0, 153.4, 136.6, 133.2, 132.9, 131.9, 129.4 (d, J = 9.0 HZ), 125.3, 124.5 (d, J = 6.0 HZ), 123.6, 118.9, 115.6, 115.4, 109.0, 55.0, 52.5, 31.6, 16.2. ESI-MS: m/z 488.5 (M+1), 510.6 (M+Na). $C_{27}H_{26}FN_5OS$

(487.18). HPLC purity: 98.44%.

3,5-Dimethyl-4-((2-((1-(4-nitrobenzyl)piperidin-4-yl)amino)thieno[3,2-d]

pyrimidin-4-yl)oxy)benzonitrile (25). Recrystallized from EA/PE as a yellow solid, 68.4% yield, mp: 157-159°C. ¹H NMR (400 MHz, DMSO-*d*₆, ppm): δ 8.19 (m, 3H), 7.72 (s, 2H, C₃,C₅-Ph''-H), 7.57 (d, *J* = 8.4 Hz, 2H, C₂,C₆-Ph'-H), 7.25 (s, 1H, C₇-thienopyrimidine-H), 6.91 (s, 1H, NH), 3.74-3.76 (m, 1H), 3.57 (s, 2H, N-CH₂), 2.73 (s, 2H), 2.11 (s, 6H), 1.78 (s, 2H), 1.40-1.44 (m, 4H). ¹³C NMR (100 MHz, DMSO-*d*₆): δ 162.4, 160.5, 153.4, 147.5, 147.0, 140.6, 136.8, 133.2, 132.9, 130.0, 129.1, 123.8, 119.0, 109.0, 61.6, 52.7, 31.7, 16.2. ESI-MS: *m/z* 515.6 (M+1), 537.6 (M+Na). C₂₇H₂₆N₆O₃S (514.18). HPLC purity: 97.93%.

3,5-Dimethyl-4-((2-((1-(4-(methylsulfonyl)benzyl)piperidin-4-yl)amino)thieno[3,2

-d]pyrimidin-4-yl)oxy)benzonitrile (26). Recrystallized from EA/PE as a white solid, 52.4% yield, mp: >300°C. ¹H NMR (400 MHz, DMSO-*d*₆, ppm): δ 8.18 (d, 1H, *J* = 5.3 Hz, C₆-thienopyrimidine-H), 7.86 (d, 2H, *J* = 8.2 Hz, C₃,C₅-Ph'-H), 7.71 (s, 2H, C₃,C₅-Ph''-H), 7.54 (d, 2H, *J* = 8.2 Hz, C₂,C₆-Ph'-H), 7.24 (s, 1H, C₇-thienopyrimidine-H), 6.88 (s, 1H, NH), 3.74-3.76 (m, 1H), 3.56 (s, 2H, N-CH₂), 3.06 (s, 3H, SO₂CH₃), 2.72-2.75 (m, 2H), 2.10 (s, 6H), 2.05-2.09 (m, 2H), 1.92 (s, 2H), 1.42-1.44 (m, 2H). ¹³C NMR (100 MHz, DMSO-*d*₆): δ 165.4, 162.7, 160.1, 153.3, 145.4, 139.1, 134.9, 133.1, 132.2, 129.6, 127.4, 123.3, 118.7, 109.5, 62.3, 52.3, 44.5, 32.0, 16.4. ESI-MS: *m/z* 548.4 (M+1), 570.5 (M+Na). C₂₈H₂₉N₅O₃S₂ (547.69). HPLC purity: 95.73%.

4-((4-((4-(4-Cyano-2,6-dimethylphenoxy)thieno[3,2-d]pyrimidin-2-yl)amino)

piperidin-1-yl)methyl)benzenesulfonamide (27). Recrystallized from EA/PE as a white solid, 50.3% yield, mp: 223-225°C. ¹H NMR (400 MHz, DMSO-*d*₆, ppm): δ 8.18 (d, *J* = 5.3 Hz, 1H, C₆-thienopyrimidine-H), 7.76 (d, *J* = 8.3 Hz, 2H, C₃,C₅-Ph'-H), 7.72 (s, 2H, C₃,C₅-Ph''-H), 7.45 (d, *J* = 8.2 Hz, 2H, C₂,C₆-Ph'-H), 7.29 (s, 2H, SO₂NH₂), 7.25 (s, 1H, C₇-thienopyrimidine-H), 6.87 (s, 1H, NH), 3.74 (s, 1H), 3.48 (s, 2H, N-CH₂), 2.72 (s, 2H), 2.10 (s, 6H), 1.95-2.04 (m, 2H), 1.77 (s, 2H), 1.40-1.45 (m, 2H). ¹³C NMR (100 MHz, DMSO-*d*₆): δ 165.9, 162.5, 160.5, 153.4, 143.3, 143.1, 136.7, 133.2, 132.9, 129.4, 126.0, 123.8, 123.7, 119.0, 109.0, 61.9, 52.8, 31.7, 16.2. ESI-MS: *m/z* 549.5 (M+1). C₂₇H₂₈N₆O₃S₂ (548.50). HPLC purity: 99.83%.

4-((2-((1-(4-Fluorobenzyl)piperidin-4-yl)amino)thieno[3,2-*d*]pyrimidin-4-yl)oxy)-3,5-dimethylbenzonitrile (28). Recrystallized from EA/PE as a white solid, 61.8% yield, mp: >300°C. ¹H NMR (400 MHz, DMSO-*d*₆, ppm): δ 7.79 (d, *J* = 5.3 Hz, 1H, C₆-thienopyrimidine-H), 7.43 (s, 2H, C₃,C₅-Ph''-H), 7.26-7.29 (m, 3H), 7.21 (s, 1H, C₇-thienopyrimidine-H), 7.03 (t, *J* = 8.4 Hz, 2H), 3.69 (s, 1H), 3.47 (s, 2H, N-CH₂), 2.72 (s, 2H), 2.12 (s, 6H), 1.78-1.89 (m, 4H), 1.39-1.43 (m, 2H). ¹³C NMR (100 MHz, DMSO-*d*₆): δ 165.4, 163.2, 160.1, 153.3, 135.0, 133.1, 132.2, 130.6, 123.3, 115.1, 114.9, 109.5, 62.1, 52.0, 31.9, 29.7, 16.4. ESI-MS: *m/z* 488.5 (M+1). C₂₇H₂₆FN₅OS (487.59). HPLC purity: 95.81%.

3,5-Dimethyl-4-((2-((1-(pyridin-4-ylmethyl)piperidin-4-yl)amino)thieno[3,2-*d*]pyrimidin-4-yl)oxy)benzonitrile (29). Recrystallized from EA/PE as a white solid, 51.3% yield, mp: 154-156°C. ¹H NMR (400 MHz, DMSO-*d*₆, ppm) δ: 8.48 (d, *J* =

5.3 Hz, 1H), 8.20 (d, J = 8.3 Hz, 2H, C₃,C₅-Ph'-H), 7.72 (s, 1H, C₇-thienopyrimidine-H), 7.57 (d, J = 8.2 Hz, 2H, C₃,C₅-Ph'-H), 7.28 (s, 2H, C₃,C₅-Ph''-H), 6.93 (s, 1H, NH), 3.74 (s, 1H), 3.48 (s, 2H, N-CH₂), 2.73 (s, 2H), 2.12 (s, 6H), 1.70-1.76 (m, 2H), 1.37-1.43 (m, 2H), 1.17-1.18 (m, 2H). ¹³C NMR (100 MHz, DMSO): δ 166.9, 162.5, 160.5, 150.1, 148.2, 144.7, 136.6, 133.2, 127.2, 124.1, 119.0, 109.0, 61.2, 52.7, 31.6, 16.2. ESI-MS: m/z 471.5 (M+1). C₂₆H₂₆N₆OS (470.59). HPLC purity: 99.47%.

4-((2-((1-(2,4-Difluorobenzyl)piperidin-4-yl)amino)thieno[3,2-d]pyrimidin-4-yl)-oxy)-3,5-dimethylbenzonitrile (30). Recrystallized from EA/PE as a white solid, 55.7% yield, mp: >300°C. ¹H NMR (400 MHz, DMSO-*d*₆, ppm): δ 7.79 (d, J = 5.6 Hz, 1H, C₆-thienopyrimidine-H), 7.43 (s, 2H, C₃,C₅-Ph''-H), 7.37 (dd, J = 15.2, 8.4 Hz, 1H), 7.27 (s, 1H, C₇-thienopyrimidine-H), 7.21 (d, J = 5.2 Hz, 1H, C₆-Ph'-H), 6.77-6.88 (m, 2H), 3.71 (s, 1H), 3.54 (s, 2H, N-CH₂), 2.74 (s, 2H), 2.11 (s, 6H), 1.33-1.84 (m, 2H), 1.35-1.42 (m, 4H). ¹³C NMR (100 MHz, DMSO-*d*₆): δ 165.4, 162.7, 160.1, 153.3, 134.9, 133.1, 132.2, 123.3, 118.7, 111.1 (dd, J = 21.0, 4.0 Hz), 109.5, 103.8 (t, J = 25.0 Hz), 54.7, 51.7, 31.9, 16.4. ESI-MS: m/z 506.3 (M+1). C₂₇H₂₅F₂N₅OS (505.17). HPLC purity: 95.46%.

3-(((4-((4-(4-Cyano-2,6-dimethylphenoxy)thieno[3,2-d]pyrimidin-2-yl)amino)piperidin-1-yl)methyl)benzenesulfonamide (31). Recrystallized from EA/PE as a white solid, 52.1% yield, mp: 212-214°C. ¹H NMR (400 MHz, DMSO-*d*₆, ppm): δ 8.20 (d, J = 4.0 Hz, 1H, C₆-thienopyrimidine-H), 7.76 (s, 1H, C₂-Ph'-H), 7.71-7.73 (m, 3H, C₄,C₅,C₆-Ph'-H), 7.50 (s, 2H, C₃,C₅-Ph''-H), 7.37 (s, 2H, SO₂NH₂), 7.27 (s, 1H,

C₇-thienopyrimidine-H), 6.92 (s, 1H, NH), 3.74 (s, 1H), 3.50 (s, 2H, N-CH₂), 2.75 (s, 2H), 2.11 (s, 6H), 1.78-1.99 (m, 4H), 1.37-1.46 (m, 2H). ¹³C NMR (100 MHz, DMSO-*d*₆): δ 164.9, 160.6, 150.1, 144.5, 140.2, 133.2, 129.2, 125.9, 124.7, 119.0, 107.9, 62.0, 52.6, 31.6, 16.2. ESI-MS: *m/z* 549.5 (M+1). C₂₇H₂₈N₆O₃S₂ (548.50). HPLC purity: 95.01%.

**N-((4-((4-((4-Cyano-2,6-dimethylphenoxy)thieno[3,2-d]pyrimidin-2-yl)amino)pipe-
peridin-1-yl)methyl)phenyl)methanesulfonamide (32).** Recrystallized from EA/PE as a white solid, 43.2% yield, mp: 241-245°C. ¹H NMR (400 MHz, DMSO-*d*₆, ppm): δ 9.92 (s, 1H, NHSO₂), 8.21 (d, *J* = 4.0 Hz, 1H, C₆-thienopyrimidine-H), 7.72 (s, 2H, C₃,C₅-Ph''-H), 7.03-7.40 (m, 6H), 3.82 (s, 1H), 3.38 (s, 2H, N-CH₂), 3.01 (s, 3H, SO₂CH₃), 2.82 (s, 2H), 2.10 (s, 6H), 1.53-1.91 (m, 6H). ¹³C NMR (100 MHz, DMSO-*d*₆): δ 172.5, 165.6, 162.5, 160.4, 153.3, 136.8, 133.2, 123.7, 119.8, 119.0, 109.0, 105.7, 60.8, 60.2, 45.7, 21.5, 16.2, 14.5, 8.9. ESI-MS: *m/z* 563.5 (M+1). C₂₈H₃₀N₆O₃S₂ (562.18). HPLC purity: 96.12%.

**4-((4-((4-((4-Cyano-2,6-dimethylphenoxy)thieno[3,2-d]pyrimidin-2-yl)amino)pipe-
ridin-1-yl)methyl)-N-methylbenzenesulfonamide (33).** Recrystallized from EA/PE as a white solid, 41.6% yield, mp: 181-184°C. ¹H NMR (400 MHz, DMSO-*d*₆, ppm): δ 8.21 (d, *J* = 4.0 Hz, 1H, C₆-thienopyrimidine-H), 7.73-7.75 (m, 4H), 7.45-7.53 (m, 3H), 7.27 (s, 1H, C₇-thienopyrimidine-H), 6.94 (s, 1H, NH), 3.76 (s, 1H), 3.37 (s, 2H, N-CH₂), 2.68-2.79 (m, 2H), 2.41(s, 6H, CH₃), 2.11(s, 6H), 1.38-1.87 (m, 6H). ¹³C NMR (100 MHz, DMSO-*d*₆): δ 162.5, 160.5, 153.4, 144.2, 140.8, 136.7, 133.2, 129.7, 127.1, 123.7, 123.6, 119.0, 110.8, 109.0, 62.0, 60.2, 56.6, 52.3, 36.4, 31.5, 29.1, 16.2.

ESI-MS: m/z 563.4 ($M+1$). $C_{28}H_{30}N_6O_3S_2$ (562.18). HPLC purity: 95.78%.

4-(((4-((4-(4-Cyano-2,6-dimethylphenoxy)thieno[3,2-d]pyrimidin-2-yl)amino)piperidin-1-yl)methyl)benzamide (34). Recrystallized from EA/PE as a white solid, 41.8% yield, mp: 218-220°C. 1H NMR (400 MHz, DMSO- d_6 , ppm): δ 8.20 (d, J = 5.2 Hz, 1H, C₆-thienopyrimidine-H), 7.93 (d, J = 8.0 Hz, 2H, C₃,C₅-Ph'-H), 7.76 (s, 2H, C₃,C₅-Ph''-H), 7.40 (d, J = 8.0 Hz, 2H, C₂,C₆-Ph'-H), 7.35 (s, 2H, CONH₂), 7.30 (s, 1H, C₇-thienopyrimidine-H), 6.94 (s, 1H, NH), 3.73 (s, 1H), 3.46 (s, 2H, N-CH₂), 2.74 (s, 2H), 2.10 (s, 6H), 1.74-1.95 (m, 4H), 1.42-1.44 (m, 2H). ^{13}C NMR (100 MHz, DMSO- d_6): δ 168.5, 162.4, 160.5, 150.2, 139.3, 136.2, 134.2, 133.5, 132.3, 128.9, 126.1, 119.4, 109.6, 62.4, 52.5, 31.5, 16.2. ESI-MS: m/z 513.3 ($M+1$). $C_{28}H_{28}N_6O_2S$ (512.20). HPLC purity: 98.69%.

3-(((4-((4-(4-Cyano-2,6-dimethylphenoxy)thieno[3,2-d]pyrimidin-2-yl)amino)piperidin-1-yl)methyl)benzamide (35). Recrystallized from EA/PE as a white solid, 57.3% yield, mp: 223-225°C. 1H NMR (400 MHz, DMSO- d_6 , ppm): δ 8.19 (d, J = 4.0 Hz, 1H, C₆-thienopyrimidine-H), 7.96 (s, 2H, C₃,C₅-Ph''-H), 7.72-7.79 (m, 4H), 7.34-7.42 (m, 3H), 7.26 (s, 1H, C₇-thienopyrimidine-H), 6.88 (s, 1H, NH), 3.73 (s, 1H), 3.46 (s, 2H, N-CH₂), 2.74 (s, 2H), 2.11 (s, 6H), 1.71-1.95 (m, 4H), 1.40-1.44 (m, 2H). ^{13}C NMR (100 MHz, DMSO- d_6): δ 168.4, 162.5, 160.5, 160.5, 150.1, 139.2, 136.6, 134.6, 133.2, 132.0, 128.4, 126.4, 119.0, 109.0, 62.4, 52.7, 31.7, 16.2. ESI-MS: m/z 513.4 ($M+1$). $C_{28}H_{28}N_6O_2S$ (512.20). HPLC purity: 98.43%.

Ethyl 4-(((4-((4-(4-cyano-2,6-dimethylphenoxy)thieno[3,2-d]pyrimidin-2-yl)amino)piperidin-1-yl)methyl)benzoate (36). Recrystallized from EA/PE as a white

solid, 73.6% yield, mp: 188-191°C. ¹H NMR (400 MHz, DMSO-*d*₆, ppm): δ 8.21 (d, *J* = 5.2 Hz, 1H, C₆-thienopyrimidine-H), 7.94 (d, *J* = 8.0 Hz, 2H, C₃,C₅-Ph'-H), 7.75 (s, 2H, C₃,C₅-Ph''-H), 7.41 (d, *J* = 8.0 Hz, 2H, C₂,C₆-Ph'-H), 7.28 (s, 1H, C₇-thienopyrimidine-H), 6.93 (s, 1H, NH), 4.28 (q, *J* = 4.0 Hz, 2H, COOCH₂), 3.73 (s, 1H), 3.50 (s, 2H, N-CH₂), 2.73 (s, 2H), 2.11 (s, 6H), 1.78-2.04 (m, 4H), 1.40-1.44 (m, 2H), 1.30 (t, *J* = 4.0 Hz, 3H, CH₃). ¹³C NMR (100 MHz, DMSO-*d*₆): δ 166.6, 162.5, 160.6, 153.5, 144.9, 133.2, 132.8, 129.5, 129.3, 128.7, 128.2, 123.5, 119.0, 109.0, 62.1, 60.2, 52.7, 52.4, 31.7, 16.2, 14.1. ESI-MS: *m/z* 542.3 (M+1). C₃₀H₃₁N₅O₃S (541.21). HPLC purity: 97.14%.

N-((4-((4-((4-(4-Cyano-2,6-dimethylphenoxy)thieno[3,2-d]pyrimidin-2-yl)amino)piperidin-1-yl)methyl)phenyl)sulfonyl)acetamide (37). Recrystallized from EA/PE as a white solid, 50.3% yield, mp: 223-225°C. ¹H NMR (400 MHz, DMSO-*d*₆, ppm): δ 8.19 (d, *J* = 4.0 Hz, 1H, C₆-thienopyrimidine-H), 7.85 (d, *J* = 4.0 Hz, 1H, C₇-thienopyrimidine-H), 7.76 (d, *J* = 8.3 Hz, 2H, C₃,C₅-Ph'-H), 7.71 (s, 2H, C₃,C₅-Ph''-H), 7.50 (d, *J* = 8.2 Hz, 2H, C₂,C₆-Ph'-H), 7.25 (s, 1H, SO₂NH), 6.90 (s, 1H, NH), 3.75 (s, 1H), 3.52 (s, 2H, N-CH₂), 2.74 (s, 2H), 2.11 (s, 6H), 2.07 (s, 3H), 1.39-1.91 (m, 6H). ¹³C NMR (100 MHz, DMSO-*d*₆): δ 162.5, 160.5, 144.1, 139.2, 133.2, 132.9, 129.6, 127.2, 119.0, 110.1, 109.0, 61.9, 60.8, 52.7, 31.7, 24.5, 16.2. ESI-MS: *m/z* 591.5 (M+1). C₂₉H₃₀N₆O₄S₂ (590.18). HPLC purity: 99.08%.

4-(Mesityloxy)-N-(1-(4-(methylsulfonyl)benzyl)piperidin-4-yl)thieno[3,2-d]pyrimidin-2-amine (38). Recrystallized from EA/PE as a white solid, 57.4% yield, mp: 92-95°C. ¹H NMR (400 MHz, CDCl₃, ppm): δ 7.87 (d, *J* = 8.3 Hz, 2H,

C₃,C₅-Ph'-H), 7.70 (d, *J* = 5.4 Hz, 1H, C₆-thienopyrimidine-H), 7.53 (d, *J* = 8.1 Hz, 2H, C₂,C₆-Ph'-H), 7.16 (d, *J* = 5.4 Hz, 1H, C₇-thienopyrimidine-H), 6.90 (s, 2H, C₃,C₅-Ph''-H), 5.02 (s, 1H, NH), 3.58 (s, 2H, N-CH₂), 3.06 (s, 3H, SO₂-CH₃), 2.74-2.76 (m, 2H), 2.32 (s, 3H, C₄-Ph''-CH₃), 1.93-2.09 (m, 11H), 1.42-1.51 (m, 2H). ¹³C NMR (100 MHz, CDCl₃): δ 164.8, 163.6, 160.4, 147.2, 145.3, 139.1, 135.3, 134.7, 130.7, 129.7, 129.0, 127.3, 123.0, 62.3, 52.3, 44.5, 32.0, 20.9, 16.4. ESI-MS: *m/z* 537.6 (M+1), 559.5 (M+Na). C₂₈H₃₂N₄O₃S₂ (536.19). HPLC purity: 99.16%.

4-(((4-(Mesityloxy)thieno[3,2-d]pyrimidin-2-yl)amino)piperidin-1-yl)methyl)

benzoate (39). Recrystallized from EA/PE as a white solid, 52.7% yield, mp: 97-100°C. ¹H NMR (400 MHz, CDCl₃, ppm): δ 7.97 (d, *J* = 8.2 Hz, 2H, C₃,C₅-Ph'-H), 7.70 (d, *J* = 5.4 Hz, 1H, C₆-thienopyrimidine-H), 7.39 (d, *J* = 8.1 Hz, 2H, C₂,C₆-Ph'-H), 7.17 (d, *J* = 5.6 Hz, 1H, C₇-thienopyrimidine-H), 6.90 (s, 2H, C₃,C₅-Ph''-H), 5.10 (s, 1H, NH), 3.53 (s, 2H, N-CH₂), 2.73-2.76 (m, 2H), 2.31 (s, 3H, COOCH₃), 1.91-2.09 (m, 14H), 1.41-1.49 (m, 2H). ¹³C NMR (100 MHz, CDCl₃): δ 176.2, 167.0, 166.3, 164.6, 160.4, 160.0, 147.3, 143.6, 135.2, 134.6, 133.6, 132.8, 131.5, 130.7, 129.7, 129.5, 129.0, 122.9, 62.5, 52.0, 31.8, 20.8, 16.3. ESI-MS: *m/z* 517.6 (M+1), 533.5 (M+Na). C₂₉H₃₂N₄O₃S (516.22). HPLC purity: 98.49%.

N-(1-(4-Fluorobenzyl)piperidin-4-yl)-4-(mesityloxy)thieno[3,2-d]pyrimidin-2-amine (40).

Recrystallized from EA/PE as a white solid, 65.3% yield, mp: 131-136°C. ¹H NMR (400 MHz, CDCl₃, ppm): δ 7.71 (d, *J* = 5.4 Hz, 1H, C₆-thienopyrimidine-H), 7.28-7.29 (m, 2H), 7.17 (d, *J* = 5.4 Hz, 1H, C₇-thienopyrimidine-H), 7.02 (t, *J* = 8.6 Hz, 2H), 6.90 (s, 2H, C₃,C₅-Ph''-H), 4.86 (s, 1H, NH), 3.50 (s, 2H, N-CH₂), 2.73-2.78

(m, 2H), 2.32 (s, 3H, C₄-Ph''-CH₃), 1.94-2.09 (m, 11H), 1.40-1.51 (m, 2H). ¹³C NMR (100 MHz, CDCl₃): δ 164.9, 163.2, 160.8, 160.4, 147.3, 135.2, 134.5, 133.8, 130.7 (t, *J* = 8.0 Hz), 129.0, 123.0, 115.1 (d, *J* = 21.0 Hz), 62.2, 52.0, 31.9, 20.9, 16.4. ESI-MS: *m/z* 477.5 (M+1). C₂₇H₂₉FN₄OS (476.20). HPLC purity: 99.42%.

N-(1-(3-Fluorobenzyl)piperidin-4-yl)-4-(mesityloxy)thieno[3,2-d]pyrimidin-2-amine (41).

Recrystallized from EA/PE as a white solid, 63.1% yield, mp: 140-142°C. ¹H NMR (400 MHz, CDCl₃, ppm): δ 7.68 (d, *J* = 5.4 Hz, 1H, C₆-thienopyrimidine-H), 7.37 (t, *J* = 6.1 Hz, 1H, C₅-Ph'-H), 7.22 (t, *J* = 6.0 Hz, 1H, C₄-Ph'-H), 7.17 (d, *J* = 5.3 Hz, 1H, C₇-thienopyrimidine-H), 7.10 (t, *J* = 7.4 Hz, 1H, C₆-Ph'-H), 7.03 (t, *J* = 9.5 Hz, 1H, C₂-Ph'-H), 6.88 (s, 2H, C₃,C₅-Ph''-H), 5.05 (s, 1H, NH), 3.57 (s, 2H, N-CH₂), 2.78-2.80 (m, 2H), 2.31 (s, 3H, C₄-Ph''-CH₃), 1.92-2.08 (m, 11H), 1.41-1.48 (m, 2H). ¹³C NMR (100 MHz, CDCl₃): δ 165.0, 162.6, 160.5, 160.1, 147.3, 135.2, 134.4, 131.6 (d, *J* = 4.0 Hz), 130.7, 129.0, 128.7, 123.8 (d, *J* = 4.0 Hz), 123.1, 115.3 (d, *J* = 22.0 Hz), 55.2, 51.9, 32.0, 20.8, 16.4. ESI-MS: *m/z* 477.5 (M+1). C₂₇H₂₉FN₄OS (476.20). HPLC purity: 97.54%.

3-(((4-(Mesityloxy)thieno[3,2-d]pyrimidin-2-yl)amino)piperidin-1-yl)methyl) benzonitrile (42).

Recrystallized from EA/PE as a white solid, 63.5% yield, mp: 99-102°C. ¹H NMR (400 MHz, CDCl₃, ppm): δ 7.72 (d, *J* = 5.4 Hz, 1H, C₆-thienopyrimidine-H), 7.64 (s, 1H, C₂-Ph'-H), 7.58 (t, *J* = 9.0 Hz, 2H, C₄-Ph'-H), 7.44 (t, *J* = 7.7 Hz, 1H, C₅-Ph'-H), 7.17 (d, *J* = 5.3 Hz, 1H, C₇-thienopyrimidine-H), 6.90 (s, 2H, C₃,C₅-Ph''-H), 5.14 (s, 1H, NH), 3.51 (s, 2H, N-CH₂), 2.72-2.75 (m, 2H), 2.32 (s, 3H, C₄-Ph''-CH₃), 2.09 (s, 9H), 2.93 (s, 2H), 1.42-1.50 (m, 2H). ¹³C NMR

(100 MHz, CDCl₃): δ 164.8, 163.6, 160.4, 147.2, 140.2, 135.3, 134.6, 133.3, 132.4, 130.7, 129.0, 122.9, 119.0, 112.3, 62.1, 52.2, 32.0, 20.9, 16.4. ESI-MS: *m/z* 484.6 (M+1), 506.5 (M+Na). C₂₈H₂₉N₅OS (483.21). HPLC purity: 96.77%.

4-(Mesityloxy)-N-(1-(pyridin-4-ylmethyl)piperidin-4-yl)thieno[3,2-d]pyrimidin-2-amine (43). Recrystallized from EA/PE as a white solid, 50.7% yield, mp: 135-137°C.

¹H NMR (400 MHz, CDCl₃, ppm): δ 8.54 (d, *J* = 5.9 Hz, 2H, C₂,C₆-pyridine-H), 7.71 (d, *J* = 5.4 Hz, 1H, C₆-thienopyrimidine-H), 7.28 (d, *J* = 6.6 Hz, 2H, C₃,C₅-pyridine-H), 7.18 (d, *J* = 5.4 Hz, 1H, C₇-thienopyrimidine-H), 6.90 (s, 2H, C₃,C₅-Ph''-H), 4.86 (s, 1H, NH), 3.50 (s, 2H, N-CH₂), 2.74-2.77 (m, 2H), 2.32 (s, 3H, C₄-Ph''-CH₃), 1.95-2.09 (m, 11H), 1.44-1.52 (m, 2H). ¹³C NMR (100 MHz, CDCl₃): δ 164.9, 163.5, 160.4, 149.7, 147.9, 147.2, 135.2, 134.5, 130.7, 129.0, 123.8, 123.1, 106.6, 61.8, 52.3, 48.1, 32.0, 20.9, 16.4. ESI-MS: *m/z* 460.6 (M+1), 482.6 (M+Na). C₂₆H₂₉N₅OS (459.21). HPLC purity: 98.73%.

N-(1-(2,4-Difluorobenzyl)piperidin-4-yl)-4-(mesityloxy)thieno[3,2-d]pyrimidin-2-amine (44). Recrystallized from EA/PE as a white solid, 59.6% yield, mp: 110-112°C.

¹H NMR (400 MHz, CDCl₃, ppm): δ 7.70 (d, *J* = 5.4 Hz, 1H, C₆-thienopyrimidine-H), 7.36 (dd, *J* = 15.1, 8.3 Hz, 1H, C₅-Ph'-H), 7.17 (d, *J* = 5.3 Hz, 1H, C₇-thienopyrimidine-H), 6.90 (s, 2H, C₃,C₅-Ph''-H), 6.75-6.85 (m, 2H), 4.89 (d, *J* = 7.3 Hz, 1H, NH), 3.52 (s, 2H, N-CH₂), 2.75-2.78 (m, 2H), 2.32 (s, 3H, C₄-Ph''-CH₃), 2.09-2.17 (m, 9H), 1.93-1.95 (m, 2H), 1.39-1.47 (m, 2H). ¹³C NMR (100 MHz, CDCl₃): δ 165.0, 163.5, 160.4, 147.2, 135.3, 134.5, 132.4, 132.3, 132.3, 132.2, 130.7, 129.0, 123.1, 111.1 (dd, *J* = 21.0, 4.0 HZ), 103.8 (t, *J* = 25.0 HZ), 54.7, 51.8, 32.0,

20.8, 16.4. ESI-MS: m/z 495.5 (M+1), 517.6 (M+Na). $C_{27}H_{28}F_2N_4OS$ (494.20). HPLC purity: 97.20%.

4-(((4-(Mesityloxy)thieno[3,2-d]pyrimidin-2-yl)amino)piperidin-1-yl)methyl)benzamide (45).

Recrystallized from EA/PE as a white solid, 52.4% yield, mp: 192-195°C. 1H NMR (400 MHz, DMSO- d_6 , ppm): δ 8.12 (d, J = 5.4 Hz, 1H, C₆-thienopyrimidine-H), 7.93 (s, 1H), 7.82 (d, J = 8.3 Hz, 2H, C₃,C₅-Ph'-H), 7.33 (d, J = 8.1 Hz, 2H, C₂,C₆-Ph'-H), 7.22 (d, J = 5.4 Hz, 1H, C₇-thienopyrimidine-H), 6.94 (s, 2H, C₃,C₅-Ph''-H), 6.84 (s, 1H, NH), 5.76 (s, 1H, NH), 3.72 (s, 1H), 3.46 (s, 2H, N-CH₂), 2.74-2.76 (m, 2H), 2.26 (s, 3H, C₄-Ph''-CH₃), 2.02 (s, 6H, C_{2,5}-Ph''-CH₃), 1.95-1.84 (m, 4H), 1.44-1.52 (m, 2H). ^{13}C NMR (100 MHz, DMSO- d_6): δ 168.2, 163.2, 160.8, 147.3, 142.5, 136.1, 135.1, 133.4, 130.4, 129.5, 128.8, 127.8, 62.2, 56.5, 55.3, 52.7, 31.8, 31.1, 20.8, 19.0, 16.4. ESI-MS: m/z 502.3 (M+1). $C_{28}H_{31}N_5O_2S$ (501.22). HPLC purity: 97.64%.

3-(((4-(Mesityloxy)thieno[3,2-d]pyrimidin-2-yl)amino)piperidin-1-yl)methyl)benzamide (46).

Recrystallized from EA/PE as a white solid, 42.7% yield, mp: 175-177°C. 1H NMR (400 MHz, DMSO- d_6 , ppm): δ 7.91 (d, J = 8.3 Hz, 2H, C₃,C₅-Ph'-H), 7.59 (d, J = 16.0 Hz, 1H, C₆-thienopyrimidine-H), 7.48 (s, 2H, CONH₂), 7.40 (d, J = 8.1 Hz, 2H, Ph'-H), 7.34 (d, J = 4.0 Hz, 1H, Ph'-H), 7.24 (d, J = 5.4 Hz, 1H, C₇-thienopyrimidine-H), 7.08 (s, 1H), 6.41 (s, 1H, NH), 3.72 (s, 1H), 3.47 (s, 2H, N-CH₂), 2.74-2.76 (m, 2H), 2.29 (s, 3H, C₄-Ph''-CH₃), 2.08 (s, 6H, C₂,C₅-Ph''-CH₃), 1.42-1.76 (m, 6H). ^{13}C NMR (100 MHz, DMSO- d_6): δ 166.1, 162.6, 159.3, 150.5, 144.8, 131.7, 129.5, 129.2, 129.0, 119.3, 118.9, 96.6, 62.2, 61.0, 52.7,

31.6, 16.5, 14.6. ESI-MS: m/z 502.4 (M+1). $C_{28}H_{31}N_5O_2S$ (501.22). HPLC purity: 96.75%.

4-((4-((4-(Mesityloxy)thieno[3,2-d]pyrimidin-2-yl)amino)piperidin-1-yl)methyl)benzenesulfonamide (47). Recrystallized from EA/PE as a white solid, 52.3% yield, mp: 210-212°C. 1H NMR (400 MHz, DMSO- d_6 , ppm): δ 8.19 (d, J = 5.3 Hz, 1H, C₆-thienopyrimidine-H), 7.77 (d, J = 8.3 Hz, 2H, C₃,C₅-Ph'-H), 7.72 (s, 2H, C₃,C₅-Ph''-H), 7.46 (d, J = 8.2 Hz, 2H, C₂,C₆-Ph'-H), 7.30 (s, 2H, SO₂NH₂), 7.25 (s, 1H, C₇-thienopyrimidine-H), 6.81 (s, 1H, NH), 3.94 (s, 1H), 3.52 (s, 2H, N-CH₂), 2.65 (s, 2H), 2.29 (s, 3H, C₄-Ph''-CH₃), 2.10 (s, 6H), 1.59-1.83 (m, 6H). ^{13}C NMR (100 MHz, DMSO- d_6): δ 165.9, 162.5, 160.5, 153.4, 143.3, 143.1, 136.7, 133.2, 132.9, 129.4, 126.0, 123.8, 123.7, 119.0, 109.0, 61.9, 52.8, 31.7, 16.2. ESI-MS: m/z 549.5 (M+1). $C_{27}H_{28}N_6O_3S_2$ (548.50). HPLC purity: 96.16%.

4-(Mesityloxy)-N-(1-(4-nitrobenzyl)piperidin-4-yl)thieno[3,2-d]pyrimidin-2-amine (48). Recrystallized from EA/PE as a white solid, 55.6% yield, mp: 225-227°C. 1H NMR (400 MHz, DMSO- d_6 , ppm): δ 8.18 (d, J = 8.3 Hz, 2H, C₃,C₅-Ph'-H), 8.11 (d, J = 8.0 Hz, 1H, C₆-thienopyrimidine-H), 7.55 (d, J = 8.2 Hz, 2H, C₂,C₆-Ph'-H), 7.21 (d, J = 4.0 Hz, 1H, C₇-thienopyrimidine-H), 6.93 (s, 2H, C₃,C₅-Ph''-H), 6.85 (s, 1H, NH), 3.72 (s, 1H), 3.56 (s, 2H, N-CH₂), 2.73 (s, 2H), 2.26 (s, 3H, C₄-Ph''-CH₃), 2.02 (s, 6H), 1.76-1.91 (m, 4H), 1.46 (s, 2H). ^{13}C NMR (100 MHz, DMSO- d_6): δ 163.2, 160.7, 147.5, 147.3, 146.9, 136.2, 135.1, 130.4, 130.0, 129.5, 123.8, 61.6, 52.7, 31.7, 20.8, 16.4. ESI-MS: m/z 504.5 (M+1). $C_{27}H_{29}N_5O_3S$ (503.20). HPLC purity: 95.31%.

***In vitro* anti-HIV activities assays**

The anti-HIV activity and cytotoxicity of the newly synthesized compounds were evaluated with WT HIV-1 (strain HIV-IIIB), double RT mutant strains of HIV-1 IIIB (RES056 and F227L/V106A), five single RT mutant strains of HIV-1 IIIB (L100I, K103N, E138K, Y181C, Y188L), and HIV-2 (strain ROD) in MT-4 cell cultures using the 3-(4,5-dimethylthiazol-2-yl)-2,5-diphenyltetrazolium bromide (MTT) method as described previously.³²⁻³⁴ At the beginning of each experiment, stock solutions (10×final concentration) of test compounds were added in 25 μ L volumes to two series of triplicate wells in order to allow simultaneous evaluation of their effects on mock- and HIV-infected cells. Using a Biomek 3000 robot (Beckman Instruments, Fullerton, CA), serial five-fold dilutions of the test compounds (final 200 μ L volume per well) were made directly in flat-bottomed 96-well microtiter trays, including untreated control HIV-1 and mock-infected cell samples for each sample. HIV-1 (IIIB) and mutant HIV-1 strains (RES056, F227L/V106A, L100I, K103N, E138K, Y181C and Y188L) or HIV-2 (ROD) stock (50 μ L at 100-300 CCID₅₀) (50% cell culture infectious dose) or culture medium was added to either the infected or mock-infected wells of the microtiter tray. Mock-infected cells were used to evaluate the effect of test compounds on uninfected cells in order to assess the cytotoxicity of the compounds. Exponentially growing MT-4 cells were centrifuged for 5 min at 1000 rpm and the supernatant was discarded. The MT-4 cells were resuspended at 6×10^5 cells/mL, and 50 μ L aliquots were transferred to the microtiter tray wells. At five days after infection, the viability of mock- and HIV-infected cells was determined spectrophotometrically by means of the MTT assay.

The MTT assay is based on the reduction of yellow-colored MTT (Acros Organics, Geel, Belgium) by mitochondrial dehydrogenase of metabolically active cells to form a blue-purple formazan that can be measured spectrophotometrically. The absorbances were read in an eight-channel computer-controlled photometer (Multiscan Ascent Reader, Labsystems, Helsinki, Finland), at the wavelengths of 540 and 690 nm. All data were calculated using the median optical density (OD) value of three wells. The 50% effective antiviral concentration (EC_{50}) was defined as the concentration of the test compound affording 50% protection from viral cytopathogenicity. The 50% cytotoxic concentration (CC_{50}) was defined as the compound concentration that reduced the absorbance (OD_{540}) of mock-infected cells by 50%.

Recombinant HIV-1 reverse transcriptase (RT) inhibitory assays

The HIV-1 RT inhibition assay was conducted by using an RT assay kit produced by Roche. All the reagents for performing the RT reaction are contained in the kit and the procedure for assaying HIV-1 RT inhibition (recombinant WT and K103N/Y181C double-mutant RT enzymes) was performed as described in the kit protocol.³⁵

Briefly, the reaction mixture containing HIV-1 RT enzyme, reconstituted template and viral nucleotides [digoxigenin (DIG)-dUTP, biotin-dUTP and dTTP] in the incubation buffer with or without inhibitors was incubated for 1 h at 37°C. Then, the reaction mixture was transferred to a streptavidin-coated microtitre plate (MTP) and incubated for another 1 h at 37°C. The biotin-labeled dNTPs that were incorporated into the cDNA chain in the presence of RT were bound to streptavidin.

The unbound dNTPs were washed with washing buffer, and anti-DIG-POD was added to the MTPs.

After incubation for 1 h at 37°C, the DIG-labeled dNTPs incorporated in cDNA were bound to the anti-DIG-POD antibody. The unbound anti-DIG-PODs were washed out and the peroxide substrate (ABST) solution was added to the MTPs. The reaction mixture was incubated at 25°C until the green color was sufficiently developed for detection. The absorbance of the sample was determined at OD₄₀₅ nm using a microtiter plate ELISA reader. The percentage inhibitory activity of RT inhibitors was calculated according to the following formula:

$$\% \text{ Inhibition} = \frac{[\text{O.D. value with RT but without inhibitors} - \text{O.D. value with RT and inhibitors}]}{[\text{O.D. value with RT and inhibitors} - \text{O.D. value without RT and inhibitors}]}$$

The IC₅₀ values correspond to the concentrations of the inhibitors required to inhibit biotin-dUTP incorporation by 50%.

Molecular simulations

Molecular modelling was performed with the Tripos molecular modelling packages Sybyl-X 2.0. All the molecules for docking were built using standard bond lengths and angles from Sybyl-X 2.0/Base Builder and were optimized using the Tripos force field for 1000 generations two times or more, until the minimized conformers of the ligand were the same. The flexible docking method (Surflex-Dock) docks the ligand automatically into the ligand-binding site of the receptor by using a protocol-based approach and an empirically derived scoring function. The protocol is

a computational representation of a putative ligand that binds to the intended binding site and is a unique and essential element of the docking algorithm. The scoring function in Surflex-Dock, containing hydrophobic, polar, repulsive, entropic, and solvation terms, was trained to estimate the dissociation constant (K_d) expressed as $-\log(K_d)^2$. The protein was prepared by removing the ligand, water molecules and other unnecessary small molecules from the crystal structure of the ligand HIV-1 RT complex (PDB code: 3M8Q) before docking; polar hydrogen atoms and charges were added to the protein. Surflex-Dock default settings were used for other parameters, such as the maximum number of rotatable bonds per molecule (set to 100), and the maximum number of poses per ligand (set to 20). During the docking procedure, all of the single bonds in residue side-chains inside the defined RT binding pocket were regarded as rotatable or flexible, and the ligand was allowed to rotate at all single bonds and to move flexibly within the tentative binding pocket. The atomic charges were recalculated using the Kollman all-atom approach for the protein and the Gasteiger-Hückel approach for the ligand. The binding interaction energy was calculated, including van der Waals, electrostatic, and torsional energy terms defined in the Tripos force field. The structure optimization was performed for 10,000 generations using a genetic algorithm, and the 20-best-scoring ligand-protein complexes were kept for further analysis. The $-\log(K_d)^2$ values of the 20-best-scoring complexes, representing the binding affinities of ligand with RT, encompassed a wide range of functional classes (10^{-2} - 10^{-9}). Therefore, only the highest-scoring 3D structural model of ligand-bound RT was chosen to define the binding interaction.

Pharmacokinetics study assays

Ten male Sprague-Dawley rats were randomly divided into two groups to receive the low dosage level (8 mg.kg⁻¹) or the medium dosage level (16 mg.kg⁻¹). **27** solution was prepared by dissolving **27** in a mixture of polyethylene glycol (peg) 400/normal saline (70/30, V/V) before the experiment. Both dosages were administered to rats by gavage. Blood samples were collected from the sinus jugularis into heparinized centrifugation tubes at 5 min, 15 min, 30 min, 1 h, 2 h, 4 h, 6 h, 8h, 12 h, 14 h, and 24 h after dosing. The samples were then centrifuged at 2200g for 8 min to separate plasma, which was stored at -20°C until analysis. LC-MS analysis was used to determine the concentration of **27** in plasma. Briefly, 50 µL of plasma was added to 50 µL of internal standard and 300 µL of methanol in a 5 mL centrifugation tube, which was centrifuged at 3000g for 10 min. The supernatant layer was collected and a 20 µL aliquot was injected for LC-MS analysis. Standard curves for **27** in blood were generated by the addition of various concentrations of **27** together with internal standard to blank plasma. All samples were quantified with an Agilent 1200 LC/MSD (Agilent, USA). The mobile phase was methanol/1.5% glacial acetic acid (50:50, V/V) at a flow rate of 1.0 mL/min and the test wavelength was 225 nm. All blood samples were centrifuged in an Eppendorf 5415D centrifuge and quantified by Agilent 1200 LC/MSD (Agilent, USA).

Acute toxicity experiment

The Kunming mice (18-22 g) were purchased from the animal experimental center of Shandong University. The sample **27** was suspended in PEG-400 in

concentrations of $100 \text{ mg} \cdot \text{mL}^{-1}$ and $200 \text{ mg} \cdot \text{mL}^{-1}$ respectively, and the mice were fasting for 12 hours before administered intragastrically. Then the 2 groups of mice were tested in the dose of $1000 \text{ mg} \cdot \text{kg}^{-1}$ and $2000 \text{ mg} \cdot \text{kg}^{-1}$, and 6 mice in half respectively male and female were used per group in the same dose.

AUTHOR INFORMATION

Corresponding Authors

*C.P.: e-mail, christophe.pannecouque@rega.kuleuven.be; phone, 32-(0)16-332171;

*P.Z.: e-mail, zhanpeng1982@sdu.edu.cn; phone, 086-531-88382005;

*X.L.: e-mail, xinyongl@sdu.edu.cn; phone, 086-531-88380270.

Notes

The authors declare no competing financial interest.

The authors declare for the adherence to the guidelines on animal studies (care and use of laboratory animals).

ACKNOWLEDGMENTS

Financial support from the National Natural Science Foundation of China (NSFC Nos. 81273354, 81573347), Key Project of NSFC for International Cooperation (Nos. 81420108027, 30910103908), Young Scholars Program of Shandong University (YSPSDU No. 2016WLJH32, to P.Z.), the Science and Technology Development Project of Shandong Province (No. 2014GSF118175, 2014GSF118012), Major Project of Science and Technology of Shandong Province (No. 2015ZDJS04001) and KU Leuven (GOA 10/014) is gratefully acknowledged. We thank K. Erven, K. Uyttersprot and C. Heens for technical assistance with the HIV assays.

ABBREVIATIONS USED

AIDS, acquired immunodeficiency syndrome; CC₅₀, 50% cytotoxicity concentration; DAPY, diarylpyrimidine; EC₅₀, the concentration causing 50% inhibition of antiviral activity; HAART, highly active antiretroviral therapy; HIV, human immunodeficiency virus; NRTIs, nucleoside reverse transcriptase inhibitors; NNRTI, non-nucleoside reverse transcriptase inhibitors; RT, reverse transcriptase; SAR, structure-activity relationship; SI, selection index; WT, wild-type; NVP, nevirapine; DLV, delavirdine; EFV, efavirenz; ETV, etravirine; RPV, rilpivirine; AZT, azidothymidine.

Supporting Information Available: HPLC conditions, Tables for HPLC data of target compounds, fold-resistance of compounds **26–48** (except **30**) against HIV-1 mutant strains respect to wild type HIV-1 strain. This material is available free of charge via the Internet at <http://pubs.acs.org>.

REFERENCES

- (1) Shattock, R. J.; Warren, M.; McCormack, S.; Hankins, C. A. AIDS. Turning the tide against HIV. *Science* **2011**, 333, 42–43.
- (2) Zhan, P.; Pannecouque, C.; De Clercq, E.; Liu, X. Anti-HIV drug discovery and development: Current innovations and future trends. *J. Med. Chem.* **2016**, 59, 2849–2878.
- (3) Hartman, T. L.; Buckheit, R. W, Jr. The continuing evolution of HIV-1 therapy: identification and development of novel antiretroviral agents targeting viral and cellular targets. *Mol. Biol. Int.* **2012**, 2012, 401965.
- (4) Esté, J. A.; Cihlar, T. Current status and challenges of antiretroviral research and

therapy. *Antiviral. Res.* **2010**, *85*, 25–33.

(5) Cane, P. A.; Johnson, A. P. New developments in HIV drug resistance. *J Antimicrob. Chemother.* **2009**, *64 Suppl 1*, i37–40.

(6) (a) Li, D.; Zhan, P.; De Clercq, E.; Liu, X. Strategies for the design of HIV-1 nonnucleoside reverse transcriptase inhibitors: lessons from the development of seven representative paradigms. *J. Med. Chem.* **2012**, *55*, 3595–3613. (b) Zhan, P.; Chen, X.; Li, D.; Fang, Z.; De Clercq, E.; Liu, X. HIV-1 NNRTIs: structural diversity, pharmacophore similarity, and implications for drug design. *Med. Res. Rev.* **2013**, *33 Suppl 1*, E1–72. (c) Zhan, P.; Liu, X.; Li, Z. Recent advances in the discovery and development of novel HIV-1 NNRTI platforms: 2006-2008 update. *Curr. Med. Chem.* **2009**, *16*, 2876–2889. (d) Song, Y.; Fang, Z.; Zhan, P.; Liu, X. Recent advances in the discovery and development of novel HIV-1 NNRTI platforms (Part II): 2009-2013 update. *Curr. Med. Chem.* **2014**, *21*, 329–355. (e) Zhan, P.; Liu, X. Novel HIV-1 non-nucleoside reverse transcriptase inhibitors: a patent review (2005 - 2010). *Expert Opin. Ther. Pat.* **2011**, *21*, 717–796. (f) Li, X.; Zhang, L.; Tian, Y.; Song, Y.; Zhan, P.; Liu, X. Novel HIV-1 non-nucleoside reverse transcriptase inhibitors: a patent review (2011-2014). *Expert Opin. Ther. Pat.* **2014**, *24*, 1199–1227

(7) de Béthune, M. P. Non-nucleoside reverse transcriptase inhibitors (NNRTIs), their discovery, development, and use in the treatment of HIV-1 infection: a review of the last 20 years (1989-2009). *Antiviral. Res.* **2010**, *85*, 75–90.

(8) (a) Wensing, A. M.; Calvez, V.; Günthard, H. F.; Johnson, V. A.; Paredes, R.; Pillay, D.; Shafer, R. W.; Richman, D. D. 2015 Update of the drug resistance mutations in

HIV-1. *Top. Antivir. Med.* **2015**, *23*, 132–141. (b) Wensing, A. M.; Calvez, V.; Günthard, H. F.; Johnson, V. A.; Paredes, R.; Pillay, D.; Shafer, R. W.; Richman, D. D. 2014 Update of the drug resistance mutations in HIV-1. *Top. Antivir. Med.* **2014**, *22*, 642–650.

(9) Richman, D.; Shih, C. K.; Lowy, I.; Rose, J.; Prodanovich, P.; Goff, S.; Griffin, J. Human immunodeficiency virus type 1 mutants resistant to nonnucleoside inhibitors of reverse transcriptase arise in tissue culture. *Proc. Natl. Acad. Sci. U.S.A.* **1991**, *88*, 11241–11245.

(10) (a) Chen, X.; Zhan, P.; Li, D.; De Clercq, E.; Liu, X. Recent advances in DAPYs and related analogues as HIV-1 NNRTIs. *Curr. Med. Chem.* **2011**, *18*, 359–376. (b) Bart, L.; De, Corte. From 4,5,6,7-tetrahydro-5-methylimidazo[4,5,1-jk](1,4)benzodiazepin-2(1H)-one (TIBO) to etravirine (TMC125): Fifteen years of research on non-nucleoside inhibitors of HIV-1 reverse transcriptase. *J. Med. Chem.* **2005**, *48*, 1689–1696. (c) Lansdon, E. B.; Brendza, K. M.; Hung, M.; Wang, R.; Mukund, S.; Jin, D.; Birkus, G.; Kutty, N.; Liu, X. Crystal structures of HIV-1 reverse transcriptase with etravirine (TMC125) and rilpivirine (TMC278): implications for drug design. *J. Med. Chem.* **2010**, *53*, 4295–4299.

(11) Nel, A.; Bekker, L. G.; Bukusi, E.; Hellström, E.; Kotze, P.; Louw, C.; Martinson, F.; Masenga, G.; Montgomery, E.; Ndaba, N.; van der Straten, A.; van Niekerk, N.; Woodsong, C. Safety, acceptability and adherence of dapivirine vaginal ring in a microbicide clinical trial conducted in multiple countries in sub-Saharan Africa. *PLoS*

One **2016**, *11*, e0147743.

(12) (a) Das, K.; Clark, A. D. Jr.; Lewi, P. J.; Heeres, J.; De Jonge, M. R.; Koymans L. M.; Vinkers, H. M.; Daeyaert, F.; Ludovici, D. W.; Kukla, M. J.; De Corte, B.; Kavash, R. W.; Ho, C. Y.; Ye, H.; Lichtenstein, M. A.; Andries, K.; Pauwels, R.; De Béthune, M. P.; Boyer, P. L.; Clark, P.; Hughes, S. H.; Janssen, P. A.; Arnold, E. Roles of conformational and positional adaptability in structure-based design of TMC125-R165335 (etravirine) and related non-nucleoside reverse transcriptase inhibitors that are highly potent and effective against wild-type and drug-resistant HIV-1 variants. *J. Med. Chem.* **2004**, *47*, 2550–2560. (b) Das, K.; Bauman, J. D.; Clark, A. D. Jr.; Frenkel, Y. V.; Lewi, P. J.; Shatkin, A. J.; Hughes, S. H.; Arnold, E. High-resolution structures of HIV-1 reverse transcriptase/TMC278 complexes: strategic flexibility explains potency against resistance mutations. *Natl. Acad. Sci. U.S.A.* **2008**, *105*, 1466–1471. (c) Das, K.; Arnold, E. HIV-1 reverse transcriptase and antiviral drug resistance. Part 1. *Curr. Opin. Virol.* **2013**, *3*, 111–118. (d) Das, K.; Arnold, E. HIV-1 reverse transcriptase and antiviral drug resistance. Part 2. *Curr. Opin. Virol.* **2013**, *3*, 119–128.

(13) Minudo, J. J.; Haubrich, R. Etravirine: a second-generation NNRTI for treatment-experienced adults with resistant HIV-1 infection. *Future HIV Ther.* **2008**, *2*, 525–537.

(14) Rimsky, L.; Vingerhoets, J.; Van Eygen, V.; Eron, J.; Clotet, B.; Hoogstoel, A.; Boven, K.; Picchio, G. Genotypic and phenotypic characterization of HIV-1 isolates obtained from patients on rilpivirine therapy experiencing virologic failure in the

phase 3 ECHO and THRIVE studies: 48-week analysis. *J. Acquired Immune Defic. Syndr.* **2012**, *59*, 39–46.

(15) Zhan, P.; Liu, X.; Li, Z.; Pannecouque, C.; De Clercq, E. Design strategies of novel NNRTIs to overcome drug resistance. *Curr. Med. Chem.* **2009**, *16*, 3903–3917.

(16) Kertesz, D. J.; Brotherton-Pleiss, C.; Yang, M.; Wang, Z.; Lin, X.; Qiu, Z.; Hirschfeld, D. R.; Gleason, S.; Mirzadegan, T.; Dunten, P. W.; Harris S. F.; Villaseñor A. G.; Hang, J. Q.; Heilek, G. M.; Klumpp, K. Discovery of piperidin-4-yl-aminopyrimidines as HIV-1 reverse transcriptase inhibitors. N-benzyl derivatives with broad potency against resistant mutant viruses. *Bioorg. Med. Chem. Lett.* **2010**, *20*, 4215–4218.

(17) Tang, G.; Kertesz, D. J.; Yang, M.; Lin, X.; Wang, Z.; Li, W.; Qiu, Z.; Chen, J.; Mei, J.; Chen, L.; Mirzadegan, T.; Harris, S. F.; Villaseñor, A. G.; Fretland, J.; Fitch, W. L.; Hang, J. Q.; Heilek, G.; Klumpp, K. Exploration of piperidine-4-yl-aminopyrimidines as HIV-1 reverse transcriptase inhibitors. N-Phenyl derivatives with broad potency against resistant mutant viruses. *Bioorg. Med. Chem. Lett.* **2010**, *20*, 6020–6023.

(18) Song, Y.; Zhan, P.; Li, X.; Rai, D.; De Clercq, E.; Liu, X. Multivalent agents: a novel concept and preliminary practice in Anti-HIV drug discovery. *Curr. Med. Chem.* **2013**, *20*, 815–832.

(19) (a) Chen, X.; Zhan, P.; Liu, X.; Cheng, Z.; Meng, C.; Shao, S.; Pannecouque, C.; De Clercq, E.; Liu, X. Design, synthesis, anti-HIV evaluation and molecular modeling of piperidine-linked amino-triazine derivatives as potent non-nucleoside reverse

transcriptase inhibitors. *Bioorg. Med. Chem.* **2012**, *20*, 3856–3864. (b) Chen, X.; Li, Y.; Ding, S.; Balzarini, J.; Pannecouque, C.; De Clercq, E.; Liu, H.; Liu, X. Discovery of piperidine-linked pyridine analogues as potent non-nucleoside HIV-1 reverse transcriptase inhibitors. *ChemMedChem* **2013**, *8*, 1117–1126. (c) Zhang, L.; Zhan, P.; Chen, X.; Li, Z.; Xie, Z.; Zhao, T.; Liu, H.; De Clercq, E.; Pannecouque, C.; Balzarini, J.; Liu, X. Design, synthesis and preliminary SAR studies of novel N-arylmethyl substituted piperidine-linked aniline derivatives as potent HIV-1 NNRTIs. *Bioorg. Med. Chem.* **2014**, *22*, 633–642.

(20) Gunaydin, H.; Bartberger, M. D. Stacking with no planarity? *ACS Med. Chem. Lett.* **2016**, *7*, 341–344.

(21) (a) Ekkati, A. R.; Bollini, M.; Domaoal, R. A.; Spasov, K. A.; Anderson, K. S.; Jorgensen, W. L. Discovery of dimeric inhibitors by extension into the entrance channel of HIV-1 reverse transcriptase. *Bioorg. Med. Chem. Lett.* **2012**, *22*, 1565–1568. (b) Bollini, M.; Cisneros, J. A.; Spasov, K. A.; Anderson, K. S.; Jorgensen, W. L. Optimization of diarylazines as anti-HIV agents with dramatically enhanced solubility. *Bioorg. Med. Chem. Lett.* **2013**, *23*, 5213–5216. (c) Bollini, M.; Frey, K. M.; Cisneros, J. A.; Spasov, K. A.; Das, K.; Bauman, J. D.; Arnold, E.; Anderson, K. S.; Jorgensen, W. L. Extension into the entrance channel of HIV-1 reverse transcriptase--crystallography and enhanced solubility. *Bioorg. Med. Chem. Lett.* **2013**, *23*, 5209–5212.

(22) La Regina, G.; Coluccia, A.; Brancale, A.; Piscitelli, F.; Gatti, V.; Maga, G.; Samuele, A.; Pannecouque, C.; Schols, D.; Balzarini, J.; Novellino, E.; Silvestri, R.

Indolylarylsulfones as HIV-1 non-nucleoside reverse transcriptase inhibitors: new cyclic substituents at indole-2-carboxamide. *J. Med. Chem.* **2011**, *54*, 1587–1598.

(23) Liu, N.; Wei, L.; Huang, L.; Yu, F.; Zheng, W.; Qin, B.; Zhu, D. Q.; Morris-Natschke, S. L.; Jiang, S.; Chen, C. H.; Lee, K. H.; Xie, L. Novel HIV-1 non-nucleoside reverse transcriptase inhibitor agents: Optimization of diarylanilines with high potency against wild-type and rilpivirine-resistant E138K mutant virus. *J. Med. Chem.* **2016**, *59*, 3689–3704.

(24) (a) Meng, Q.; Chen, X.; Kang, D.; Huang, B.; Li, W.; Zhan, P.; Daelemans, D.; De Clercq, E.; Pannecouque, C.; Liu, X. Design, synthesis and evaluation of novel HIV-1 NNRTIs with dual structural conformations targeting the entrance channel of the NNRTI binding pocket. *Eur. J. Med. Chem.* **2016**, *115*, 53–62. (b) Yang, J.; Chen, W.; Kang, D.; Lu, X.; Li, X.; Liu, Z.; Huang, B.; Daelemans, D.; Pannecouque, C.; De Clercq, E.; Zhan, P.; Liu, X. Design, synthesis and anti-HIV evaluation of novel diarylpyridine derivatives targeting the entrance channel of NNRTI binding pocket. *Eur. J. Med. Chem.* **2016**, *109*, 294–304. (c) Chen, X.; Meng, Q.; Qiu, L.; Zhan, P.; Liu, H.; De Clercq, E.; Pannecouque, C.; Liu, X. Design, synthesis, and anti-HIV evaluation of novel triazine derivatives targeting the entrance channel of the NNRTI binding pocket. *Chem. Biol. Drug Des.* **2015**, *86*, 122–128. (d) Liu, Z.; Chen, W.; Zhan, P.; De Clercq, E.; Pannecouque, C.; Liu, X. Design, synthesis and anti-HIV evaluation of novel diarylnicotinamide derivatives (DANAs) targeting the entrance channel of the NNRTI binding pocket through structure-guided molecular hybridization. *Eur. J. Med. Chem.* **2014**, *87*, 52–62.

- (25) (a) Tian, Y.; Du, D.; Rai, D.; Wang, L.; Liu, H.; Zhan, P.; De Clercq, E.; Pannecouque, C.; Liu, X. Fused heterocyclic compounds bearing bridgehead nitrogen as potent HIV-1 NNRTIs. Part 1: design, synthesis and biological evaluation of novel 5,7-disubstituted pyrazolo[1,5-a]pyrimidine derivatives. *Bioorg. Med. Chem.* **2014**, *22*, 2052–2059. (b) Wang, L.; Tian, Y.; Chen, W.; Liu, H.; Zhan, P.; Li, D.; Liu, H.; De Clercq, E.; Pannecouque, C.; Liu, X. Fused heterocycles bearing bridgehead nitrogen as potent HIV-1 NNRTIs. Part 2: discovery of novel [1,2,4]Triazolo[1,5-a]pyrimidines using a structure-guided core-refining approach. *Eur. J. Med. Chem.* **2014**, *85*, 293–303. (c) Huang, B.; Li, C.; Chen, W.; Liu, T.; Yu, M.; Fu, L.; Sun, Y.; Liu, H.; De Clercq, E.; Pannecouque, C.; Balzarini, J.; Zhan, P.; Liu, X. Fused heterocycles bearing bridgehead nitrogen as potent HIV-1 NNRTIs. Part 3: optimization of [1,2,4]triazolo[1,5-a]pyrimidine core via structure-based and physicochemical property-driven approaches. *Eur. J. Med. Chem.* **2015**, *92*, 754–65. (d) Huang, B.; Liang, X.; Li, C.; Chen, W.; Liu, T.; Li, X.; Sun, Y.; Fu, L.; Liu, H.; De Clercq, E.; Pannecouque, C.; Zhan, P.; Liu, X. Fused heterocycles bearing bridgehead nitrogen as potent HIV-1 NNRTIs. Part 4: design, synthesis and biological evaluation of novel imidazo[1,2-a]pyrazines. *Eur. J. Med. Chem.* **2015**, *93*, 330–337. (e) Chen, W.; Zhan, P.; Daelemans, D.; Yang, J.; Huang, B.; De Clercq, E.; Pannecouque, C.; Liu, X. Structural optimization of pyridine-type DAPY derivatives to exploit the tolerant regions of the NNRTI binding pocket. *Eur. J. Med. Chem.* **2016**, *121*, 352–363.
- (26) Frey, K. M.; Bollini, M.; Mislak, A. C.; Cisneros, J. A.; Gallardo-Macias, R.; Jorgensen, W. L.; Anderson, K. S. Crystal structures of HIV-1 reverse transcriptase

with picomolar inhibitors reveal key interactions for drug design. *J. Am. Chem. Soc.* **2012**, *134*, 19501–19503.

(27) Janssen, P. A.; Lewi, P. J.; Arnold, E.; Daeyaert, F.; de Jonge, M.; Heeres, J.; Koymans, L.; Vinkers, M.; Guillemont, J.; Pasquier, E.; Kukla, M.; Ludovici, D.; Andries, K.; de Béthune, M. P.; Pauwels, R.; Das, K.; Clark, A. D. Jr.; Frenkel, Y. V.; Hughes, S. H.; Medaer, B.; De Knaep, F.; Bohets, H.; De Clerck, F.; Lampo, A.; Williams, P.; Stoffels, P. In search of a novel anti-HIV drug: multidisciplinary coordination in the discovery of 4-[[4-[[4-[(1E)-2-cyanoethenyl]-2,6-dimethylphenyl]amino]-2-pyrimidinyl]amino]benzonitrile (R278474, rilpivirine). *J. Med. Chem.* **2005**, *48*, 1901–1909.

(28) Sergeyev, S.; Yadav, A. K.; Franck, P.; Michiels, J.; Lewi, P.; Heeres, J.; Vanham, G.; Ariën, K. K.; Vande Velde, C. M.; De Winter, H.; Maes, B. U. 2,6-Di(arylamino)-3-fluoropyridine derivatives as HIV non-nucleoside reverse transcriptase inhibitors. *J. Med. Chem.* **2016**, *59*, 1854–1868.

(29) Stumpfe, D.; Bajorath, J. Exploring activity cliffs in medicinal chemistry. *J. Med. Chem.* **2012**, *55*, 2932–2942.

(30) Stumpfe, D.; Hu, Y.; Dimova, D.; Bajorath, J. Recent progress in understanding activity cliffs and their utility in medicinal chemistry. *J. Med. Chem.* **2014**, *57*, 18–28.

(31) Carroll, S. S.; Olsen, D. B.; Bennett, C. D.; Gotlib, L.; Graham, D. J.; Condra, J. H.; Stern, A. M.; Shafer, J. A.; Kuo, L. C. Inhibition of HIV-1 reverse transcriptase by pyridinone derivatives. Potency, binding characteristics, and effect of template sequence. *J. Biol. Chem.* **1993**, *268*, 276–281.

- (32) Pauwels, R.; Balzarini, J.; Baba, M.; Snoeck, R.; Schols, D.; Herdewijn, P.; Desmyter, J.; De Clercq, E. Rapid and automated tetrazolium-based colorimetric assay for the detection of anti-HIV compounds. *J. Virol. Methods* **1988**, *20*, 309–321.
- (33) Pannecouque, C.; Daelemans, D.; De Clercq, E. Tetrazolium-based colorimetric assay for the detection of HIV replication inhibitors: revisited 20 years later. *Nat. Protoc.* **2008**, *3*, 427–434.
- (34) Zhan, P.; Liu, X.; Li, Z.; Fang, Z.; Li, Z.; Wang, D.; Pannecouque, C.; De Clercq, E. Novel 1,2,3-thiadiazole derivatives as HIV-1 NNRTIs with improved potency: Synthesis and preliminary SAR studies. *Bioorg. Med. Chem.* **2009**, *17*, 5920–5927.
- (35) Suzuki, K.; Craddock, B. P.; Okamoto N.; Kano T.; Steigbigel, R. T. Poly A-linked colorimetric microtiter plate assay for HIV reverse transcriptase. *J. Virol. Methods* **1993**, *44*, 189–198.

Table 3. Anti-HIV-1 activity of compounds 26-48 against HIV-1 mutant strains.

compd	EC ₅₀ ^a							SI ^b						
	L100I	K103N	Y181C	Y188L	E138k	F227L+ V106A	RES056	L100I	K103N	Y181C	Y188L	E138k	F227L+ V106A	RES056
26	73±39	12±5.8	36±2.9	41±7.7	39±2.8	44±5.9	442±149	306	1804	622	543	566	507	50
27	3.4±0.6	2.9	3.2±0.4	3.0±0.1	2.9	4.2±1.2	30.6±12	>159101	>67385	>78125	>70028	>75758	>78125	>53533
28	90.9±42	8.7±2.5	37.8±4.9	44.8±3.9	34.4±2.1	712±664	1073±201	1549	16227	3735	3145	4103	198	131
29	81.6±31.2	9.9±0.2	42.7±3.9	55.3±15.9	42.2±	130±3.4	651±11	253	2091	483	373	489	159	32
30	-	-	-	-	-	-	>4100	-	-	-	-	-	-	<1
31	28.4±21	≤7.6	20.9±8.5	12.8±4.3	6.5±1.0	8.5±0.7	1900	>8033	>30120	>10870	>17781	>35211	>26652	>120
32	13.6±4.7	1.9±0.5	6.9±0.2	8.2±0.5	6.9±0.3	32.2±7.5	262±53	5018	35700	9887	8869	9900	2122	261
33	4.5±2.4	1.5±0.2	4.8±2.4	6.8±1.2	6.6±0.8	4.1±0.7	32.4±5.9	972	2880	911	647	665	1091	136
34	10.8±1.6	1.8±0.2	5.3±4.6	8.6±1.1	4.5±3.7	10.7±0.6	85.8±54	8759	53773	18103	11147	21340	8855	1110
35	50.0±19	10.3±2.0	49.5±0.5	58.3±11	13.8±0.7	130.3±24	>48768	>975	>4713	>984	>836	>3511	>374	X1
36	11280±9164	511.4±57	3710±574	4670±1802	1019±120	12821±11631	>230770	>20	>446	>62	>49	>227	>20	X1
37	20.8±10	8.2±1.7	28.8±10	13.6±3.2	8.8±2.6	8.8±1.6	144.2±36	145	369	104	222	340	340	20
38	23.9±3.0	6.2±0.9	28.9±0.7	32.2±5.6	18.2±2.4	23.9±2.1	282±99	143	548	118	106	187	81	12
39	650±273	94.6±76	161.4±8.5	243.1±64	39.5±0.5	1851±724	4687±259	38	263	154	102	629	13	5
40	1214±416	91.8±26	181.5±55	715±78	166.1±12	5313±564	6262±1381	10	130	66	17	72	2	2
41	1527±255	149±1.0	252±29	599±92	172±28	3118±104	7790±564	16	165	98	41	143	8	3
42	476±204	38.7±8	193±43	143±18	50.9±5	392±16	5318	36	445	89	120	339	44	≤3
43	56.1±4	7.3±0.7	24.6±1	37.1±7	20.9±14	133.276±75.8	206±14	101	777	230	152	270	42	27

44	1239±579	163±15	660±66	787±54	174±9	6607±3162	13960	11	86	21	18	80	2	<1
45	96.1±46	8.7±0.5	42.7±4.3	42.6±3.5	21.9±5.3	107.2±12	310.1±158	60	671	135	136	265	54	18
46	399±96	93.8±30	183.1±51	234.2±32	51.0±2.2	852.2±21	7705±1643	19	81	41	32	149	9	1
47	4519±158	4937±407	4845±118	8471±197	5505±315	4547±13	>16462	4	3	3	2	3	4	<1
48	>6394	53.4±19	200.1±73	262.1±50	125.9±4.2	>6393	>6394	<1	120	32	24	51	<1	<1
NVP	2107±196	5392±3738	>15021	>15021	271±4.8	>15021	>15000	>7	>3	X1	X1	>55	X1	X1
EFV	115.5±8.3	80.1±2.6	8.2±1.0	514.8±51	5.2±0.6	348.5±58	308±164	>55	>79	>772	>12	>1220	>18	>21
ETV	5.4±2.1	2.4±0.6	15.8±2.1	20.5±2.9	14.4±2.2	29.4±7.7	17±1.8	>853	>1952	>291	>224	>318	156	>270
AZT	3.8±2.1	5.2±0.2	6.7±1.3	6.3±0.7	7.3±2.1	4.8±0.7	11.1±5.2	>1994	>1429	>1120	>1180	>1026	>1563	>675

^a EC₅₀: concentration of compound required to achieve 50% protection of MT-4 cell cultures against HIV-1-induced cytotoxicity, as determined by the MTT method.

^b CC₅₀: concentration required to reduce the viability of mock-infected cell cultures by 50%, as determined by the MTT method.

^c SI: selectivity index, the ratio of CC₅₀/EC₅₀.

Table of Contents Graphic

